

BAD and K_{ATP} channels regulate neuron excitability and epileptiform activity

Juan Ramón Martínez-François^{1*}, María Carmen Fernández-Agüera², Nidhi Nathwani¹, Carolina Lahmann¹, Veronica L Burnham¹, Nika N Danial^{1,2*}, Gary Yellen^{1*}

¹Department of Neurobiology, Harvard Medical School, Boston, United States;

²Department of Cancer Biology, Dana-Farber Cancer Institute, Boston, United States

Abstract Brain metabolism can profoundly influence neuronal excitability. Mice with genetic deletion or alteration of *Bad* (BCL-2 agonist of cell death) exhibit altered brain-cell fuel metabolism, accompanied by resistance to acutely induced epileptic seizures; this seizure protection is mediated by ATP-sensitive potassium (K_{ATP}) channels. Here we investigated the effect of BAD manipulation on K_{ATP} channel activity and excitability in acute brain slices. We found that BAD's influence on neuronal K_{ATP} channels was cell-autonomous and directly affected dentate granule neuron (DGN) excitability. To investigate the role of neuronal K_{ATP} channels in the anticonvulsant effects of BAD, we imaged calcium during picrotoxin-induced epileptiform activity in entorhinal-hippocampal slices. BAD knockout reduced epileptiform activity, and this effect was lost upon knockout or pharmacological inhibition of K_{ATP} channels. Targeted BAD knockout in DGNs alone was sufficient for the antiseizure effect in slices, consistent with a 'dentate gate' function that is reinforced by increased K_{ATP} channel activity.

DOI: <https://doi.org/10.7554/eLife.32721.001>

***For correspondence:**

juan_martinez-francois@hms.harvard.edu (JRM-F);

Nika_Danial@dfci.harvard.edu (NND);

gary_yellen@hms.harvard.edu (GY)

Competing interests: The authors declare that no competing interests exist.

Funding: See page 19

Received: 11 October 2017

Accepted: 12 January 2018

Published: 25 January 2018

Reviewing editor: Richard Aldrich, The University of Texas at Austin, United States

© Copyright Martínez-François et al. This article is distributed under the terms of the [Creative Commons Attribution License](https://creativecommons.org/licenses/by/4.0/), which permits unrestricted use and redistribution provided that the original author and source are credited.

Introduction

Epilepsy is a very common neurological disorder in need of better therapies. Approximately one third of epilepsy patients are resistant to pharmacological treatments, and most of the current therapies can produce very severe side effects. One very effective alternative treatment is a very low carbohydrate, high fat diet—the ketogenic diet (Hartman et al., 2007; Neal et al., 2009; Thiele, 2003). On a ketogenic diet, fatty acids are converted to the ketone bodies β -hydroxybutyrate and acetoacetate, which circulate at millimolar concentrations in the blood. These ketone bodies provide an alternative fuel to tissues, including the brain (DeVivo et al., 1978; Mergenthaler et al., 2013; Owen et al., 1967; Zielke et al., 2009). The observation that increased ketone body metabolism produces seizure protection suggests that fuel utilization and neuronal excitability are linked, however, the mechanisms underlying this link are poorly understood (Bough and Rho, 2007). Some of the mechanisms proposed to underlie this metabolic seizure protection include changes in gene expression associated with decreases in glycolysis (Garriga-Canut et al., 2006; Stafstrom et al., 2009), glutamate release reduction (Juge et al., 2010), adenosine signaling through A1 purinergic receptors (Masino et al., 2011), regulation of excitability by the activity of lactate dehydrogenase (Sada et al., 2015), more efficient production of GABA from glutamate (Yudkoff et al., 2008, 2007), stimulation of mitochondrial biogenesis (Bough et al., 2006), general 'positive' shifts in energy balance (Bough et al., 2006; DeVivo et al., 1978; Pan et al., 1999), increase of GABAergic tonic inhibition through neurosteroids (Forte et al., 2016), and a decrease in neuronal excitability mediated by metabolically sensitive ATP-sensitive potassium channels (Giménez-Cassina et al., 2012).

To study how brain metabolism can modify neuronal excitability we have used a non-dietary approach to alter brain fuel utilization. The protein BAD (BCL-2 agonist of cell death) regulates both apoptosis and glucose metabolism (Giménez-Cassina and Danial, 2015). When BAD's metabolic function is disrupted by genetic alteration in mice, neurons and astrocytes display decreased glucose and increased ketone body metabolism. These effects on brain metabolism produced by BAD alteration are reminiscent of those observed with a ketogenic diet. In fact, BAD-altered mice are also strongly resistant to behavioral and electrographic seizures. At the cellular level, BAD modifications that decrease glucose metabolism produce a marked increase in the activity of ATP-sensitive potassium (K_{ATP}) channels located in dentate granule neurons (DGNs). Thus, K_{ATP} channels in the dentate gyrus, a region that is thought to limit input into the hippocampus acting as a seizure 'gate,' are well poised to mediate the effects of BAD on DGN excitability. Indeed, when K_{ATP} channels are genetically ablated, seizure resistance produced by BAD modification is abolished (Giménez-Cassina et al., 2012).

In this study, we asked if BAD can effectively alter neuronal and network excitability by opening K_{ATP} channels. In BAD knockout mice, we restored BAD expression in a fraction of the DGNs, and tested individual cells to learn whether BAD could regulate K_{ATP} channel activity in a cell-autonomous manner. We also tested the consequences of altered K_{ATP} channel activity for excitability of individual DGNs, which we measured using perforated patch recordings in the presence or absence of the K_{ATP} channel inhibitor glibenclamide. Finally, to study the anticonvulsant effect of BAD in the entorhinal-hippocampal (EC-HC) circuit, we provoked epileptiform activity by partially blocking GABA_A-mediated inhibition with picrotoxin, and monitored the activity using imaging of the calcium sensor GCaMP6f. BAD ablation reduced the epileptiform activity of the EC-HC circuit, and this seizure-protective effect depended on the presence of functional K_{ATP} channels. Furthermore, this in vitro seizure protection was reproduced by BAD deletion solely in DGNs, reinforcing the notion of the dentate gyrus as a seizure gate.

Results

The effect of BAD on K_{ATP} channels is cell-autonomous

To test whether the effects of BAD on K_{ATP} channels are cell-autonomous, we reconstituted BAD expression in the hippocampus of *Bad*^{-/-} mice through intracranial injection of an adeno-associated virus (AAV). In addition to *Bad*, the AAV also contained the sequence for the red fluorescent protein mCherry to label transduced cells. To assess the effect of BAD on neuronal K_{ATP} channels, we performed whole-cell patch-clamp experiments using an intracellular solution with a high ATP concentration (4 mM) (Figure 1A). We have previously shown that *Bad* deletion produces an increase in K_{ATP} channel activity (Giménez-Cassina et al., 2012). This increase is manifested at the whole-cell level as an initial K_{ATP} conductance that gradually decreases over the first few minutes of recording after break-in, as the intracellular solution is dialyzed with a sufficiently high ATP concentration to inhibit the initially open K_{ATP} channels; we have called this phenomenon 'washdown' (Giménez-Cassina et al., 2012). In wild-type DGNs, because K_{ATP} channels display a very low basal open probability ($NP_o = 0.05\%$), intracellular solution replacement with high ATP has no effect, so whole-cell conductance in this case remains unchanged after break-in, that is, washdown is absent in wild-type DGNs.

If BAD modification leads to an increase in K_{ATP} channel activity in DGNs in a cell-autonomous manner, washdown is expected in unlabeled *Bad*^{-/-} cells but not in mCherry-labeled BAD-reconstituted *Bad*^{-/-} cells. Indeed, *Bad*^{-/-} DGN whole-cell conductance displayed a gradual decrease during the first minute after break-in and then remained unchanged (Figure 1B). In contrast, BAD-reconstituted *Bad*^{-/-} DGNs did not display washdown (Figure 1—figure supplement 1). We also performed control experiments with low ATP (0.3 mM) in the pipette solution to measure the maximal activatable K_{ATP} conductance. In this case, if cells are not adversely affected by the overexpression of BAD and/or mCherry, *Bad*^{-/-} and BAD reconstituted *Bad*^{-/-} DGNs should display normal K_{ATP} channel current 'run-up' as channels become disinhibited when ATP is dialyzed out of the cell. Indeed, both transduced and untransduced cells displayed increases of K_{ATP} conductance of similar magnitudes (Figure 1—figure supplement 2) showing that the change in K_{ATP} currents is not due to a change in channel number, but rather to a change in channel open probability. This experiment

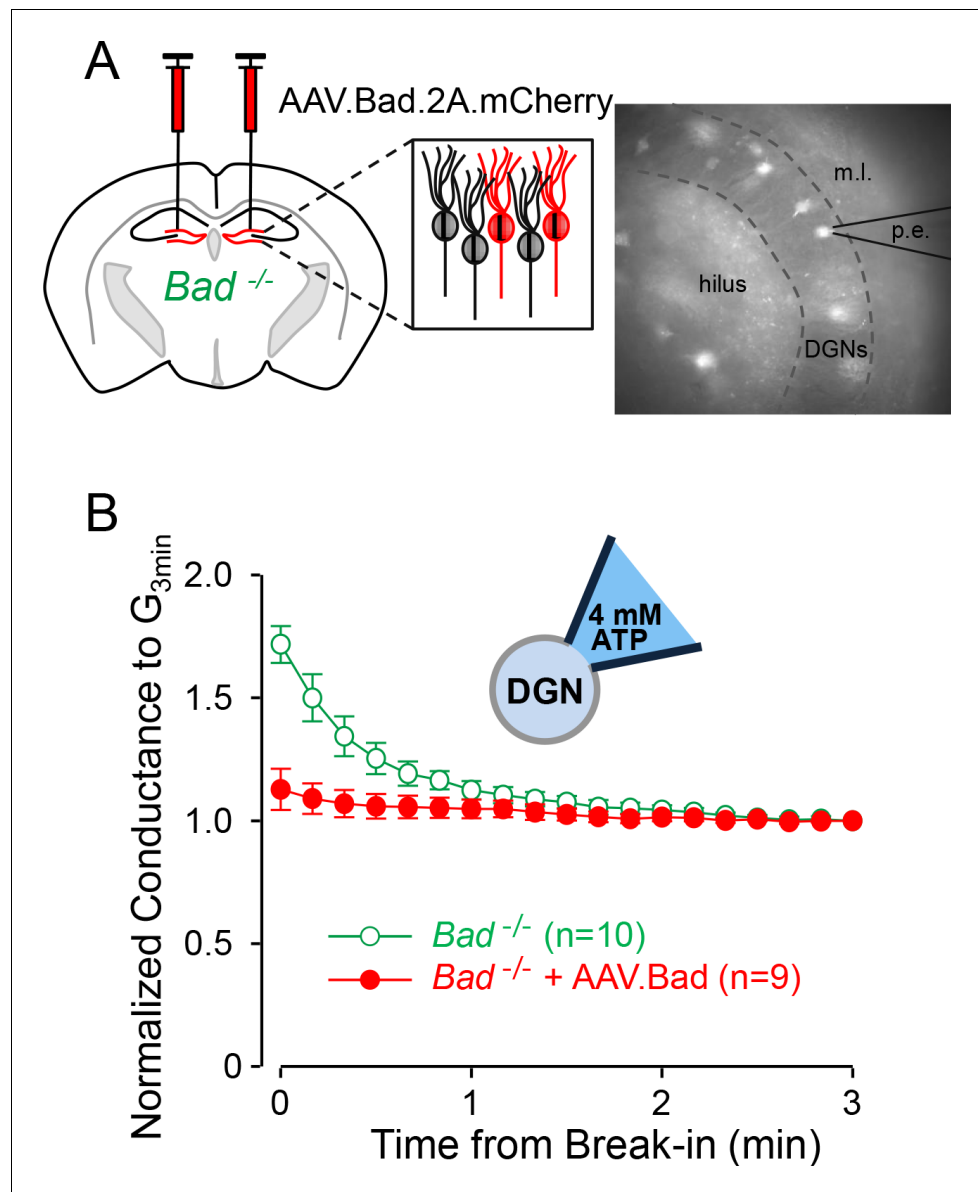


Figure 1. Effect of BAD on K_{ATP} channels is cell-autonomous. (A) Left: schematic representation of intracranial injection of AAV.Bad.2A.mCherry in the hippocampus of *Bad*^{-/-} mice to reconstitute BAD expression in mCherry labeled cells. Right: epifluorescence picture of a BAD-reconstituted *Bad*^{-/-} DGN being recorded with a patch electrode (p.e.) in the whole-cell mode. Regions observed in picture: hilus, dentate granule cell layer (DGNs) and molecular layer (m.l.). (B) ‘Washdown’ of an initially high K_{ATP} conductance, with high ATP (4 mM) in the patch electrode, seen in *Bad*^{-/-} but not BAD-reconstituted *Bad*^{-/-} cells. The time course of slope conductance measured during whole-cell recording was normalized to the value 3 min after break-in. Data are presented as mean \pm SEM.

DOI: <https://doi.org/10.7554/eLife.32721.002>

The following figure supplements are available for figure 1:

Figure supplement 1. ‘Washdown’ of K_{ATP} channel conductance in *Bad*^{-/-} or BAD-reconstituted DGNs.

DOI: <https://doi.org/10.7554/eLife.32721.003>

Figure supplement 2. Total activatable whole-cell K_{ATP} conductance is mostly unaffected by overexpressing BAD in *Bad*^{-/-} DGNs.

DOI: <https://doi.org/10.7554/eLife.32721.004>

also confirms that *Bad*^{-/-} and BAD reconstituted *Bad*^{-/-} DGNs are sufficiently healthy to maintain ATP levels that keep most (if not all) of their K_{ATP} channels closed. These results indicate that BAD can modulate K_{ATP} channel activity in a cell-autonomous manner.

K_{ATP} channels acutely modulate dentate granule neuron excitability

We then asked whether modulation of K_{ATP} channel activity could produce changes in neuronal electrical excitability. To examine DGN excitability, we performed current-clamp experiments in acute hippocampal slices. To preserve intracellular ATP dynamics, we used the perforated-patch technique to prevent dialysis of the cell's intracellular medium. In response to increasing current injections, *Bad*^{-/-} DGNs generated fewer action potentials compared to wild-type DGNs (**Figure 2A,B**). Given that, in intact cells with physiological intracellular ATP levels, K_{ATP} channels are more active in *Bad*^{-/-} cells and almost completely inactive in wild-type cells, application of glibenclamide, a K_{ATP} inhibitor, should increase excitability of *Bad*^{-/-} neurons but produce minimal effects in wild-type. As predicted, after application of 200 nM glibenclamide, *Bad*^{-/-} DGNs fired more action potentials, comparable to the response of wild-type DGNs (in the absence of glibenclamide). In contrast, the number of action potentials produced by wild-type DGNs was indistinguishable in the presence or absence of glibenclamide (**Figure 2A,B**). These results provide evidence that K_{ATP} channels can regulate DGN excitability in an acute manner. Thus, deletion of BAD could produce seizure-protective effects by decreasing neuron excitability, via modulation of K_{ATP} channels.

BAD and K_{ATP} channels regulate entorhinal-hippocampal epileptiform activity

Does the decrease in neuronal excitability mediated by K_{ATP} channels translate to a decrease in excitability at the network level? We have previously shown that global *Bad* deletion produces seizure resistance in vivo (**Giménez-Cassina et al., 2012**). To gain a more profound understanding of the seizure-protective mechanisms elicited by BAD knockout, we performed experiments in acute brain slices containing both the entorhinal cortex (EC) and the hippocampus. To examine the excitability of the EC-HC network, we monitored intracellular calcium dynamics in acute EC-HC slices with the fluorescent sensor GCaMP6f delivered by AAV. We elicited seizure-like events (SLEs) by application of 2.5 μM picrotoxin, a GABA_A receptor antagonist. Seizure-like activity is notoriously challenging to elicit in acute slices using submersion chambers, due to lack of sufficient oxygenation (**Hájos et al., 2009; Hájos and Mody, 2009; Huchzermeyer et al., 2008**). To overcome this limitation, we used a double perfusion chamber in which EC-HC slices are exposed to the extracellular solution on both sides. The flow of the oxygen-saturated extracellular solution is sufficiently high (5 ml/min) to permit an adequate oxygenation of the slice and reliably elicit seizure-like events in the presence of picrotoxin (**Figure 3** and **Video 1**).

We observed GCaMP6f expression over the whole EC-HC area (**Figure 3A**) and detected clear seizure-like events throughout the slice, which for analysis we divided into three hippocampal areas: dentate gyrus and hilus (DGH), CA3, and CA1 and 2 EC areas: medial entorhinal cortex (MEC) and lateral entorhinal cortex (LEC). We applied picrotoxin after monitoring 10 min of baseline activity. Following picrotoxin application, SLEs started to appear in the five EC-HC regions mentioned (**Figure 3B**, top and **Video 1**). This behavior is consistent with previous reports that have used electrophysiological techniques to monitor epileptiform activity in the EC-HC network using various in vitro paradigms. We have also corroborated that the SLEs we observe by GCaMP6f fluorescence intensity changes ($\Delta F/F$) faithfully mirror local electrical field potentials typically observed in this preparation (**Figure 3—figure supplement 1**). To analyze $\Delta F/F$ traces, we first filtered the signal to account for baseline drift, then set a threshold above which seizure-like activity was detected, and plotted the fraction of time spent in SLEs during the time of the experiment.

Bad^{-/-} slices spent significantly less time in SLEs compared to wild-type slices (**Figure 3C**). Furthermore, the protection from picrotoxin-elicited epileptiform activity produced by BAD was abolished by genetic deletion of the pore-forming subunit of K_{ATP} channels, Kir6.2 (*Kcnj11*), or by continuous application of the K_{ATP} channel inhibitor, glibenclamide (**Figure 3C**). These observations show that *Bad* deletion prevents seizure-like activity and that K_{ATP} channels acutely mediate BAD's seizure-protective effects.

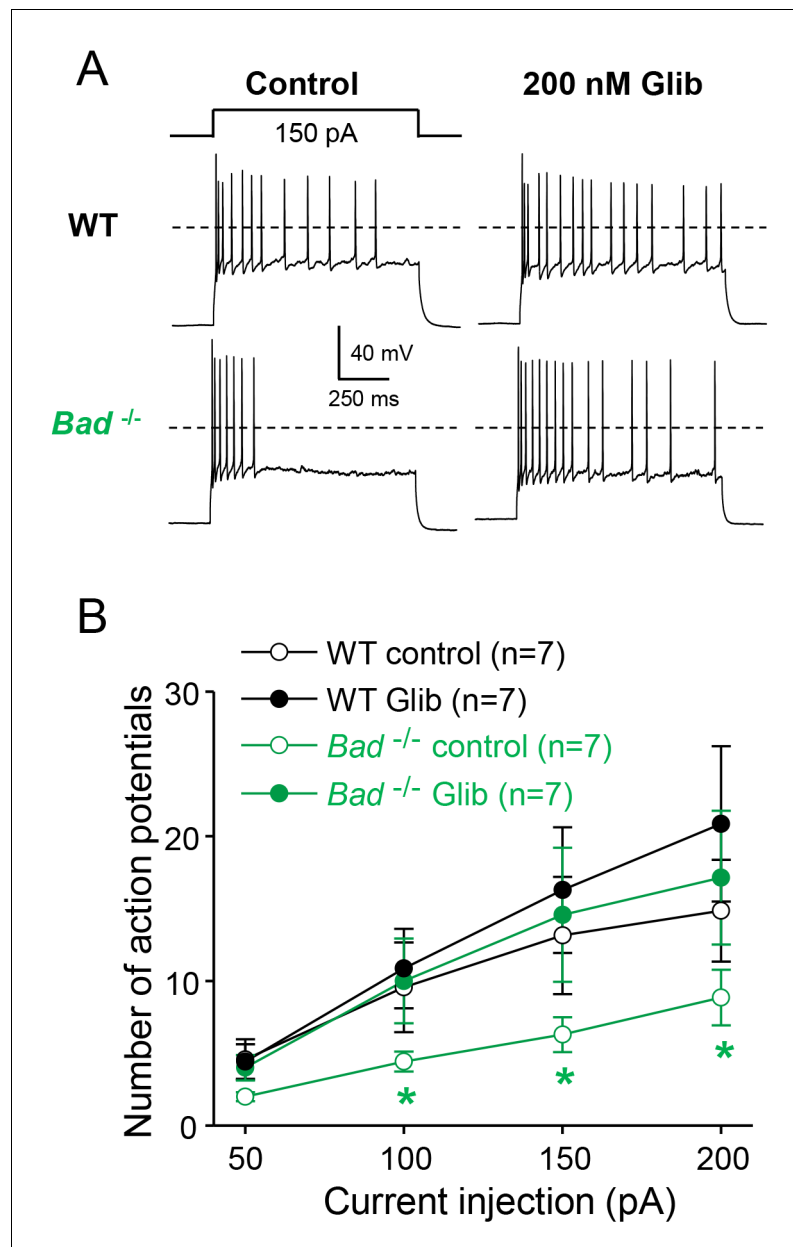


Figure 2. Dentate granule neurons lacking BAD are less excitable. (A) *Bad*^{-/-} DGNs fire fewer action potentials than wild-type (WT), and 200 nM glibenclamide reverses *Bad* knockout effect on DGN excitability. Representative perforated-patch voltage recordings in response to a 1 s, 150 pA current pulse for WT and *Bad*^{-/-} DGNs, in the presence or absence of 200 nM glibenclamide, as indicated. Dotted lines indicate 0 mV. (B) Glibenclamide application increases firing of *Bad*^{-/-} DGNs but not that of WT. Number of action potentials (mean ± SEM) plotted against magnitude of current injection pulse. **p*<0.05; 1-way ANOVA.

DOI: <https://doi.org/10.7554/eLife.32721.005>

It has been shown that long-term synaptic depression mediated by postsynaptic NMDA receptors is abolished in hippocampal slices from *Bad*^{-/-} mice (Jiao and Li, 2011). However, given that we observe no significant differences between the genotypes when K_{ATP} channels are pharmacologically inhibited or genetically deleted, our results confirm that any genotype-specific differences in glutamatergic transmission are not affecting the seizure phenotype we observe (see also Giménez-Cassina et al., 2012).

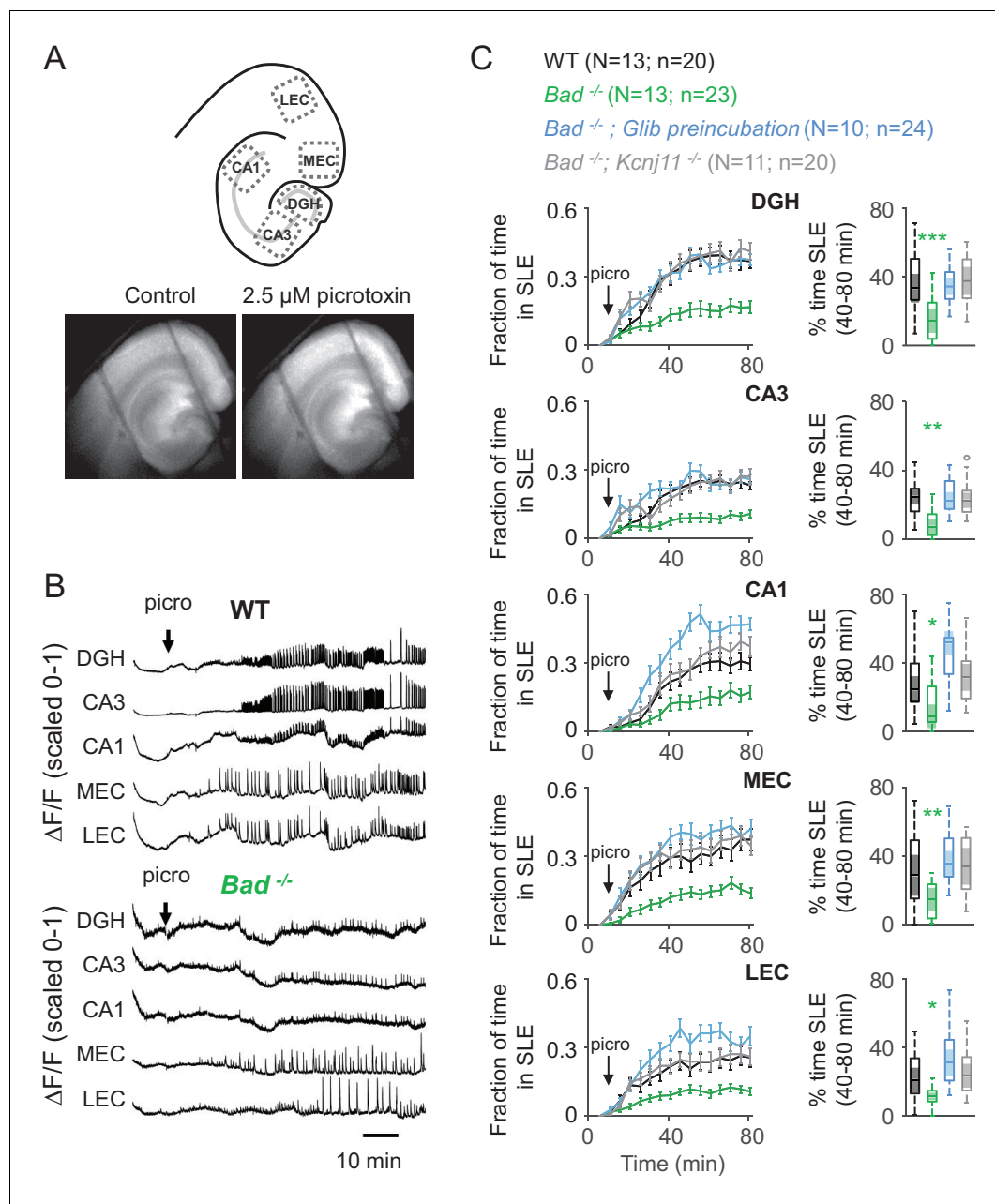


Figure 3. Deletion of BAD reduces picROTOXIN-elicited epileptiform activity. (A) Top: Schematic representation of the analyzed regions of interest in EC-HC acute slices; dentate gyrus/hilus (DGH), CA3, CA1, medial entorhinal cortex (MEC) and lateral entorhinal cortex (LEC). Bottom: representative epifluorescence images of an EC-HC slice expressing GCaMP6f in ACSF (Control; left) or in the presence of 2.5 μ M picROTOXIN as a SLE is occurring (right). (B) PicROTOXIN application triggers SLEs. Representative Δ F/F traces (normalized from 0 to 1) in wild-type (WT; top) or *Bad*^{-/-} (bottom) slices for the indicated regions of interest. The arrows indicate extracellular application of 2.5 μ M picROTOXIN in the extracellular bath. (C) Genetic deletion of BAD reduced the time EC-HC slices spent in SLEs, and this effect was mediated by K_{ATP} channels. Fraction of time spent in SLEs (mean \pm SEM) plotted versus time (left column) or percent time in SLEs calculated from the 40–80 min range when seizure-like activity plateaus (right column) for each region of interest analyzed, and genotypes and conditions specified. * p <0.05; ** p <0.005; *** p <0.0005; 1-way ANOVA. DOI: <https://doi.org/10.7554/eLife.32721.006>

The following figure supplement is available for figure 3:

Figure supplement 1. PicROTOXIN-triggered changes in GCaMP6f fluorescence intensity correspond to stereotypical epileptiform field potentials. DOI: <https://doi.org/10.7554/eLife.32721.007>

Given that BAD's antiseizure effect *in vivo* was previously demonstrated in adult mice, we wondered if BAD-dependent protection against SLEs also occurred in adult EC-HC slices. For this, we expressed GCaMP6f in the EC-HC region through AAV delivery at age P1-2 and monitored intracellular calcium in wild-type or *Bad*^{-/-} acute slices obtained at age P60-90 (**Figure 4—figure supplement 1**). In this case, a 20-fold higher picrotoxin concentration (50 μ M) was needed to elicit a roughly similar epileptiform activity in adult EC-HC slices (**Figure 4**). This may be due to diverse factors, including the maturation of the inhibitory circuits that regulate EC-HC network excitability and maturation of DGNs themselves, which become intrinsically less excitable when fully mature in adult animals. Regardless of the picrotoxin concentration needed to elicit SLEs, deletion of *Bad* also protected against SLEs in adult EC-HC slices. There was a marked decrement in time spent in SLEs in the hippocampus, though this effect was not as strong in entorhinal areas (**Figure 4**). These results corroborate the anti-SLE effects of BAD in the adult EC-HC circuit.

Targeted BAD knockout in the dentate gyrus reduces seizure-like activity

So far, we have observed that BAD knockout in the entire mouse leads to reduced excitability in brain slices; we proceeded to ask whether BAD knockout in a restricted subset of cells could reproduce this effect. The dentate gyrus has been proposed to act as seizure gate, preventing epileptiform activity initiated in the EC from passing onto other hippocampal areas such as CA3 or CA1. Therefore, it is possible that decreasing DGN excitability alone would be sufficient to 'strengthen' the dentate gyrus' gate function, and thus decrease excitability in the EC-HC circuit responsible for many types of seizures, such as in temporal lobe epilepsy.

To test if BAD deletion in DGNs alone is sufficient to produce a decrease in picrotoxin-induced SLEs, we produced conditional knockout BAD mice (*Bad*^{flox/flox}) and crossed them with transgenic mice (*Dock10-Cre*) that express Cre recombinase specifically in DGNs (*Kohara et al., 2014*). These mice (*Bad*^{flox/flox}; *Dock10-Cre*) have targeted knockout of *Bad* expression in the dentate gyrus but not in the rest of the hippocampus or EC, as confirmed by immunostaining (**Figure 5, Figure 5—figure supplement 1** and **Figure 5—figure supplement 2**). Compared to slices from both parental lines, *Bad*^{flox/flox}; *Dock10-Cre* slices (from juvenile, P13-19, mice) spent significantly less time in SLEs (**Figure 6**). Remarkably, the reduction in seizure-like activity of these slices that lack BAD solely in DGNs was comparable to that of *Bad*^{-/-} slices (compare orange *Bad*^{flox/flox}; *Dock10-Cre* and green *Bad*^{-/-} data in **Figure 6**). These results demonstrate that DGN-specific BAD knockout is sufficient to produce alleviation of seizure-like activity, supporting the idea that BAD's direct action in neurons can produce seizure protection. Furthermore, the results provide additional evidence to support the idea that the dentate gyrus acts as a gate for seizure activity.



Video 1. Seizure-like events in the presence of 2.5 μ M picrotoxin. Fluorescence intensity as imaged in **Figure 3** showing epileptiform activity in an acute EC-HP slice in the presence of 2.5 μ M picrotoxin. Video was created using ImageJ 1.51 s (Fiji).

DOI: <https://doi.org/10.7554/eLife.32721.008>

Discussion

Seizure protection can be elicited by manipulation of brain metabolism

Alterations in metabolism have long been proposed as avenues to treat epileptic seizures. One example is the ketogenic diet, which has been used for almost a century as an effective treatment for epilepsy (*Hartman et al., 2007; Neal et al., 2009; Thiele, 2003*). The switch in brain fuel metabolism from using carbohydrates to ketone bodies appears to be a major contributor to seizure protection. Compared to control animals, rats on a low-carbohydrate, high-fat diet exhibit lower glucose and increased ketone body concentrations in blood. These ketotic rats show altered brain levels of metabolites, such as the whole brain ATP/ADP ratio, suggesting an

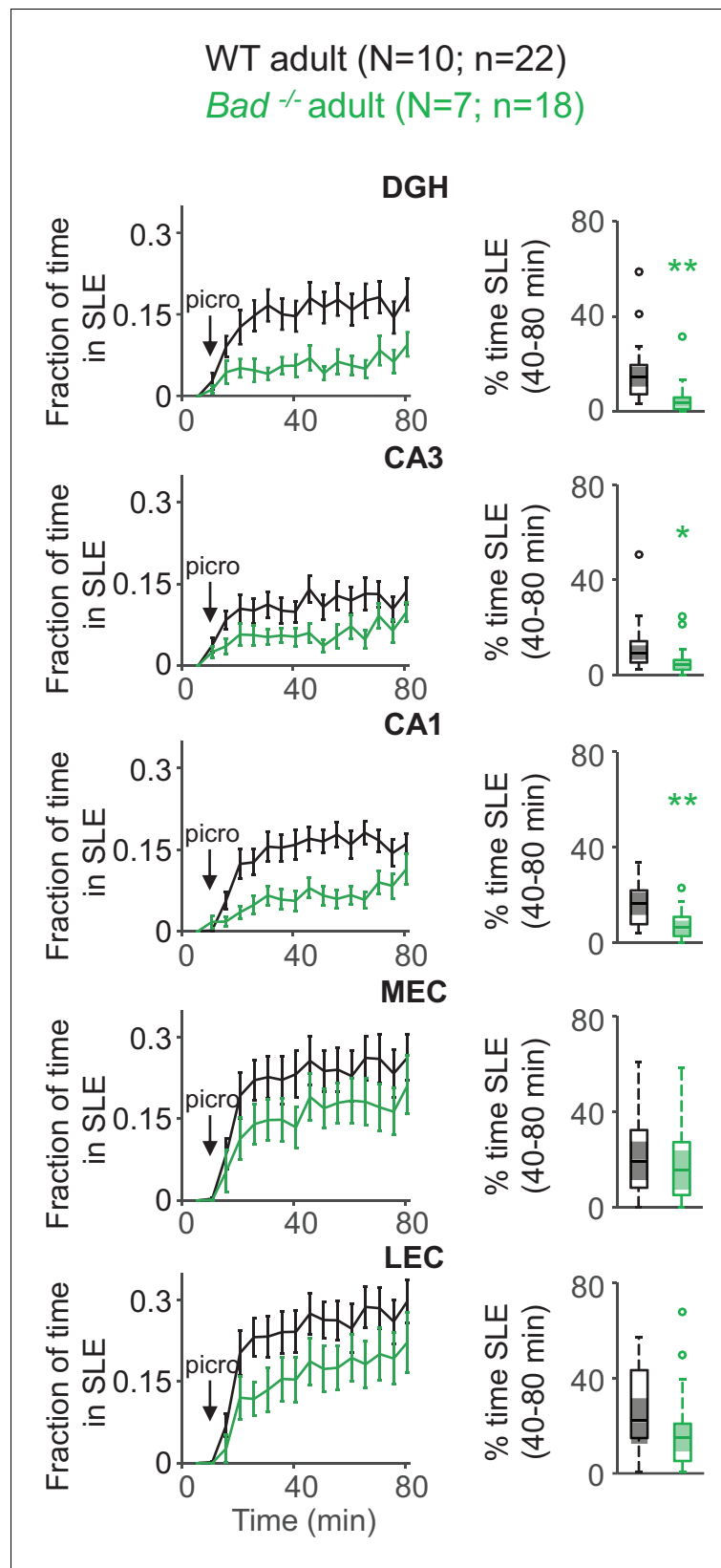


Figure 4. Deletion of BAD decreases picrotoxin-triggered seizure-like activity in adult EC-HC slices. Genetic deletion of BAD reduced the time hippocampal regions spent in SLEs in adult slices. Left column: fraction of time spent in SLEs (mean \pm SEM) plotted versus time. The arrows indicate extracellular application of 50 μ M picrotoxin
Figure 4 continued on next page

Figure 4 continued

in the extracellular bath. Right column: percent time in SLEs calculated from the 40–80 min range when seizure-like activity plateaus for each region of interest analyzed and genotypes specified. * $p < 0.05$; ** $p < 0.005$; two-tailed Student's *t*-test.

DOI: <https://doi.org/10.7554/eLife.32721.009>

The following figure supplement is available for figure 4:

Figure supplement 1. Picrotoxin-elicited epileptiform activity in adult EC-HP slices.

DOI: <https://doi.org/10.7554/eLife.32721.010>

'improved' energy state (DeVivo et al., 1978). Further, rats on the ketogenic diet upregulate transcripts encoding mitochondrial energy metabolism enzymes (Bough et al., 2006). Human patients undergoing treatment with a ketogenic diet also show changes in brain energy metabolism in agreement with rodent studies (Pan et al., 1999). The role of this metabolic switch in producing seizure protection is supported by the fact that although the anticonvulsive effect of the ketogenic diet develops gradually over days, it can be reversed in rodents and humans very rapidly upon carbohydrate consumption (Appleton and DeVivo, 1974; Huttenlocher, 1976; Pfeifer et al., 2008; Uhlemann and Neims, 1972). A different manipulation of brain metabolism by pharmacological inhibition of glycolysis also leads to seizure protection. The glycolytic inhibitor 2-deoxy-D-glucose (2DG) suppresses rodent seizures in vivo and in vitro through changes in gene expression related to epilepsy (Garriga-Canut et al., 2006; Stafstrom et al., 2009), thus reinforcing the idea that metabolic changes can produce seizure-protective effects.

Changes in metabolism mediated by BAD produce seizure resistance

We have used a *Bad*^{-/-} mouse model with effects on brain metabolism that are very reminiscent of those of the ketogenic diet; this non-dietary manipulation permits the investigation of the mechanisms involved in metabolic seizure resistance. *Bad*^{-/-} mice are resistant to acute seizures induced by either intraperitoneal injection of kainic acid, an agonist of a subclass of ionotropic glutamate receptors, or subcutaneous injection of pentylentetrazole, an antagonist of GABA_A receptors (Giménez-Cassina et al., 2012). Because these two pharmacologic models of *status epilepticus* act through different mechanisms, producing seizures with different characteristics, indicating that the seizure resistance produced by *Bad* deletion can be effective in different types of epilepsy. We have also shown that *Bad* deletion can reduce seizures and increase longevity in a genetic mouse model of epilepsy and sudden unexplained death in epilepsy (Foley et al., 2018).

BAD is a proapoptotic BCL-2 family member, but in addition to its well-known proapoptotic action, BAD also regulates glucose metabolism in various cell types (Giménez-Cassina and Danial, 2015). The switch between the apoptotic and metabolic roles of BAD occurs through phosphorylation of its serine 155 (equivalent to serine 118 in human BAD) (Danial et al., 2008). Serine 155 phosphorylation enhances glucose metabolism while inhibiting BAD's apoptotic function. Mutation of this residue to a non-phosphorylatable alanine (*Bad*^{S155A}) phenocopies the glucose-to-ketone-body fuel switch in BAD knockout neurons and astrocytes, and also produces in vivo seizure protection (Giménez-Cassina et al., 2012). Because both *Bad*^{-/-} and *Bad*^{S155A} have the same effects on K_{ATP} channel activity and seizure protection, but have opposite effects on apoptosis, the effects of BAD knockout on seizure-like activity are very likely due to BAD's effect on metabolism and not on apoptosis.

Studies in mouse models with deletions in other BCL-2 family members provide further evidence that BAD-mediated seizure protection is metabolic rather than apoptotic. Knockout of BIM or PUMA leads to neuroprotection related to seizures (Engel et al., 2011, 2010; Murphy et al., 2010). However, in contrast to our previous observations of seizure protection by BAD deletion (Giménez-Cassina et al., 2012), ablation of BIM or PUMA is not seizure protective immediately after kainic acid injection (Engel et al., 2010; Murphy et al., 2010). Instead, these other BCL-2 family members, promote hippocampal neuron death in a model of chronic seizures (intra-amygdala microinjection of kainic acid), thus, *Bim*^{-/-} or *Puma*^{-/-} animals exhibit long-term seizure protection due to decreased cell death, as opposed to *Bad*^{-/-} mice that are resistant to acute seizures due to a switch in fuel preference.

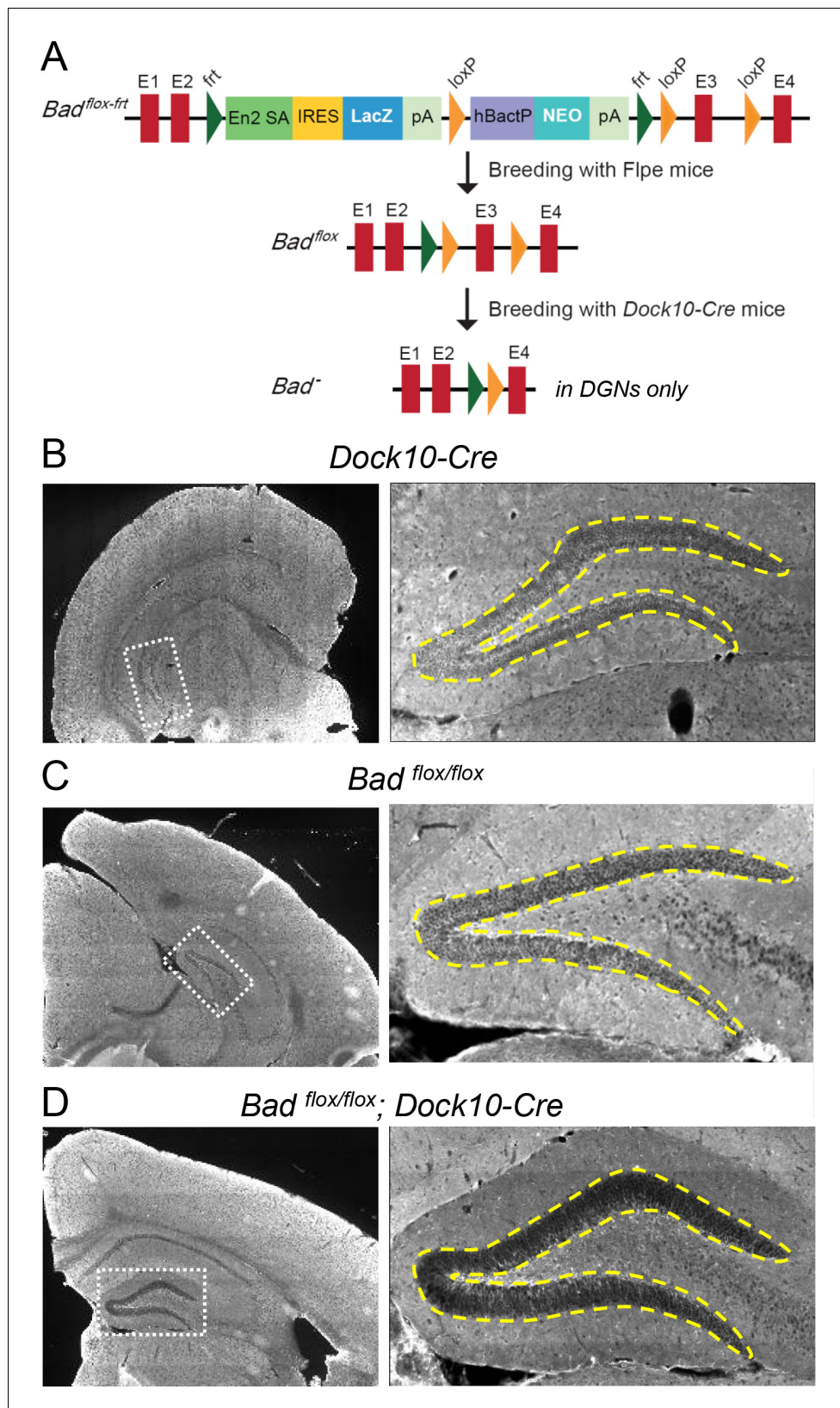


Figure 5. Targeted knockout of *Bad* expression in the dentate gyrus but not in the rest of the hippocampus. (A) Schematic illustration of the targeting construct and strategy to generate the conditional *Bad^{flox}* allele. Abbreviations: En2 SA: En2 splice acceptor; IRES: Internal ribosomal entry site; pA: polyadenylation sequence; Frt: Figure 5 continued on next page

Figure 5 continued

Flpase (Flpe) recombinase target; loxP: Cre recombinase target; hBactP: human beta actin promoter; NEO: neomycin resistance gene. (B, C, D) Immunostaining for BAD in brain coronal sections from mice of the specified genotypes. Notice lack of BAD expression only in DGNs from *Bad*^{fllox/fllox}; *Dock10-Cre* brain. In the right column dashed line area demarcates the DGN cell body layer. Also notice the lower fluorescence intensity in the entire molecular layer of the dentate gyrus (containing the dendrites of the DGNs) in *Bad*^{fllox/fllox}; *Dock10-Cre* compared to the parental genotypes.

DOI: <https://doi.org/10.7554/eLife.32721.011>

The following figure supplements are available for figure 5:

Figure supplement 1. Targeted knockout of *Bad* expression in the dentate gyrus: coronal sections.

DOI: <https://doi.org/10.7554/eLife.32721.012>

Figure supplement 2. Targeted knockout of *Bad* expression in the dentate gyrus: horizontal sections.

DOI: <https://doi.org/10.7554/eLife.32721.013>

Effects of BAD deletion are acutely mediated by K_{ATP} channels

The metabolic shift produced by BAD knockout leads to an increase in K_{ATP} channel activity. In cell-attached recordings from DGNs, where the intracellular medium—and thus ATP—is undisturbed, the open probability of K_{ATP} channels is markedly increased in *Bad*^{-/-} cells compared to wild-type cells, where these channels are mostly closed (*Giménez-Cassina et al., 2012*). Furthermore, the extra whole-cell conductance due to this increased K_{ATP} channel activity in *Bad*^{-/-} DGNs can be seen to disappear as the intracellular medium is dialyzed with an elevated ATP concentration (*Figure 1*), an effect absent in wild-type DGNs (*Giménez-Cassina et al., 2012*).

The altered K_{ATP} conductance is due to the change in open probability and not to a change in the number of functional K_{ATP} channels. In whole-cell experiments with low ATP in the intracellular medium, the maximal conductance measured after disinhibition of the channels is very similar in wild-type and *Bad*^{-/-} DGNs (*Giménez-Cassina et al., 2012*) and *Figure 1—figure supplement 2*.

Furthermore, K_{ATP} channels are required for the anti-seizure effect of *Bad* deletion. There is a reversal of seizure protection in *Bad*^{-/-} mice upon further deletion of *Kcnj11* (Kir6.2), the pore-forming subunit of neuronal K_{ATP} channels (*Giménez-Cassina et al., 2012*). More specifically, the susceptibility of *Bad*^{-/-}; *Kcnj11*^{-/-} double knockout mice to kainic acid induced seizures is comparable to that of wild-type mice, providing compelling evidence that K_{ATP} channels are required for BAD-mediated seizure resistance.

Here we found that the increased K_{ATP} conductance leads to decreased DGN excitability (*Figure 2*). Previously, K_{ATP} channels have been seen to affect neuronal excitability (*Allen and Brown, 2004; Haller et al., 2001; Pierrefiche et al., 1996*). K_{ATP} channels link metabolism to excitability because they are inhibited by intracellular ATP, and activated by intracellular ADP (*Aguilar-Bryan et al., 1998; Nichols, 2006; Proks and Ashcroft, 2009*). They are also widely expressed in the brain (*Dunn-Meynell et al., 1998; Liss and Roeper, 2001*) and are present at a particularly high density in DGNs (*Karschin et al., 1997; Mourre et al., 1991; Zawar et al., 1999*), where their single-channel activity can be readily recorded (*Giménez-Cassina et al., 2012; Pelletier et al., 2000; Tanner et al., 2011*).

The regulation of neuronal excitability by K_{ATP} channels has been extensively studied in the context of protection from hypoxia or ischemia: these channels prevent prolonged depolarizations that produce neuronal damage (*Sun and Feng, 2013; Sun et al., 2006; Yamada et al., 2001*). Additionally, they are crucial in the response of hypothalamic neurons to circulating glucose levels (*Ashford et al., 1990; Levin, 2002; Miki et al., 2001; Rowe et al., 1996; Song et al., 2001*). Our results show that K_{ATP} channels can acutely modulate DGN excitability at the cellular level (*Figure 2*) as well as network excitability in slices that are disinhibited by picrotoxin to exhibit seizure-like events (*Figure 3*). This acute pharmacological reversal of DGN excitability supports the role of neuronal K_{ATP} channels as key molecules mediating seizure protection (*Giménez-Cassina et al., 2012; Yamada et al., 2001*).

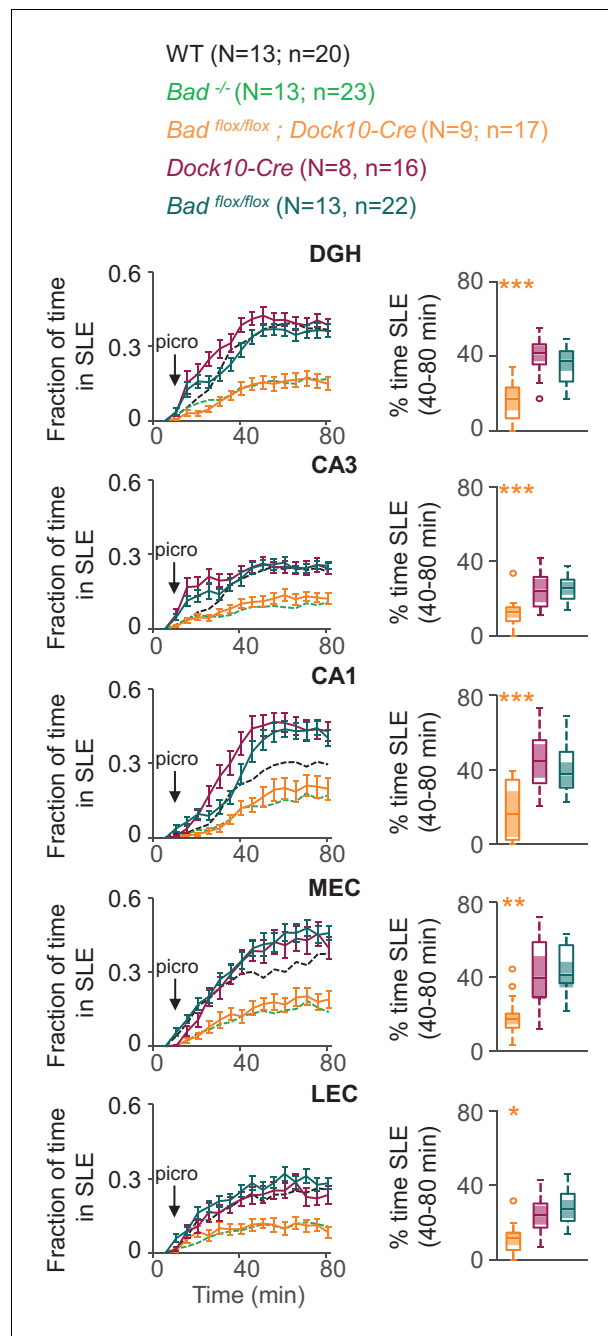


Figure 6. DGN-specific BAD ablation is sufficient to reduce seizure-like activity. Genetic deletion of *Bad* in DGNs alone (*Bad*^{flox/flox}; *Dock10-Cre*, orange) reduced the time hippocampal regions spent in SLEs in adult slices. Left column: fraction of time spent in SLEs (mean ± SEM) for *Bad*^{flox/flox}; *Dock10-Cre* (orange), *Dock10-Cre* (dark magenta) or *Bad*^{flox/flox} (teal) plotted versus time. For comparison, WT (black) and *Bad*^{-/-} (green) data are reproduced from **Figure 3** as dashed lines without error bars. Right column: percent time in SLEs calculated from the 40–80 min range when seizure-like activity plateaus for each region of interest analyzed. **p*<0.05; ***p*<0.005; ****p*<0.0005; 1-way ANOVA.

DOI: <https://doi.org/10.7554/eLife.32721.014>

Targeted *Bad* deletion in the DGNs is sufficient to produce seizure protection

We also show that eliminating *Bad* specifically in the brain can lead to changes in K_{ATP} channel activity and network excitability. When BAD was restored in single *Bad*^{-/-} DGNs via AAV, K_{ATP} channel activity reverted to that of wild-type DGNs (**Figure 1**), signifying that BAD's effect on neurons can be reversed in a cell-autonomous manner and does not seem to depend on other types of brain cells, such as astrocytes. At the network level, we show that either global knockout or DGN-targeted knockout of BAD produced a decrease in picrotoxin-induced seizure-like activity (**Figures 3 and 6**), and this effect was mediated by K_{ATP} channels. This suggests that BAD's action in specific neuronal populations may alleviate seizures. However, it is yet to be tested whether *Bad* deletion solely in DGNs produces seizure protection in vivo. Future in vivo studies involving targeted *Bad* deletion in different neuron populations are needed to pinpoint whether additional brain regions are necessary for the BAD-mediated antiseizure effect.

BAD modulates a seizure gate in the dentate gyrus

The K_{ATP} -mediated decrease in DGN excitability elicited inhibition of network excitability, consistent with the seizure protection observed in BAD-altered mice. The dentate gyrus controls the input from the entorhinal cortex into the rest of the hippocampus; ictal activity can be initiated in the EC and propagate through the dentate gyrus to CA3 and/or CA1. Furthermore, because of the recurrent connectivity of the EC-HP circuit due to the afferents from CA1 to the EC that pass through the subiculum, excitation can then re-enter the EC (**Andersen et al., 1966; Barbarosie et al., 2000; Barbarosie and Avoli, 1997; Behr et al., 1998; Spencer and Spencer, 1994; Uva et al., 2005**). In this way, the effect of the dentate gate in principle may be observed by decreased excitation not only throughout the hippocampus but also extending to the EC, as we observe in this study. Thus, limiting DGN excitability could lead to seizure protection by 'strengthening' the dentate gate. It has also been observed that ictal activity could either directly propagate from the EC to CA1 (**Ang et al., 2006**) or originate in the dentate and subsequently spread to the EC (**Lu et al., 2016; Meyer et al., 2016**). Our observations of a BAD-dependent decrease in time spent in SLEs are consistent with this picture (**Figures 3, 4 and 6**). Further, we found that *Bad* deletion specific to the dentate was sufficient to elicit protection from picrotoxin-triggered SLEs. Remarkably, EC-HC slices from mice lacking BAD exclusively in DGNs displayed a similar reduction in seizure-like activity to that of slices from mice in which BAD had been globally knocked-out (**Figure 6**).

Our immunostaining results show robust BAD knockout in DGNs (including stratum lucidum, which contains the mossy fiber projections from DGNs) of *Bad*^{flox/flox}; *Dock10-Cre* mice compared to the parental controls (**Figure 5**). This targeted *Bad* knockout had no discernable effect on BAD expression elsewhere in the brain slices we examined. We cannot rule out that very sparse expression of *Dock10-Cre* in the EC (Allen Institute Mouse Brain Atlas; expression of *Dock10*) could affect some cells, however, the absence of *Bad* throughout the DGN layer of *Bad*^{flox/flox}; *Dock10-Cre* mice, together with the substantial effect on the seizure-like activity, seems most consistent with a primary effect of the dentate acting as a seizure gate, as suggested previously from both in vitro and in vivo experiments (**Dengler and Coulter, 2016; Heinemann et al., 1992; Hsu, 2007; Krook-Magnuson et al., 2015; 2013; Lothman et al., 1992**). Interestingly, seizure-like activity is decreased in all areas (including EC) of the EC-HC slices upon BAD knockout specifically in DGNs; as previously mentioned this could reflect the recurrent nature of the EC-HC circuit where the dentate gate could decrease reentrant excitation into the EC. Taken together, these observations illuminate a mechanism by which neuronal metabolism can regulate neuronal excitability to produce seizure protection.

BAD-mediated seizure protection remains throughout brain development

Mechanisms of both seizure production and seizure protection appear to change throughout brain development (**Dengler and Coulter, 2016; Holmes and Ben-Ari, 2001**). Consistent with this, we observed that a 20-fold higher picrotoxin concentration is required to elicit robust SLEs in adult slices compared to juvenile (**Figure 4**). In the juvenile mouse brain, most DGNs are immature and still integrating into the circuit; they are more excitable than mature cells and have yet to fully develop their inhibitory connections (**Espósito et al., 2005; Mongiat and Schinder, 2011; Piatti et al.,**

2013; Schmidt-Hieber et al., 2004). Our results are also consistent with developmental changes in GABAergic signaling, including the shift from a depolarizing to a hyperpolarizing chloride current during brain maturation (Ben-Ari et al., 2012; Hollrigel et al., 1998; Liu et al., 1996; Rheims et al., 2008; Yu et al., 2013).

We also observed that in adults, BAD-mediated seizure resistance is more limited to the hippocampal region and is not as prominent in the EC (Figure 4). This pattern is consistent with BAD-mediated reinforcement of a dentate gate that limits invasion of elevated EC activity into the hippocampus. The fact that in juvenile slices, DGN-specific deletion of BAD also affected EC activity may indicate that, at the lower levels of disinhibition (lower [picrotoxin]), recurrent excitation from the hippocampus to EC is more relevant than in adult slices.

BAD knockout leads to K_{ATP} channel activation by several possible mechanisms

The detailed mechanism by which BAD knockout influences K_{ATP} channel activity is still unknown. One possibility is that although ATP in the whole brain of *Bad*^{-/-} mice is not reduced (Giménez-Cassina et al., 2012), the ATP concentration in a compartment local to the channels is reduced. Indeed, ATP consumption at the plasma membrane by the Na^+/K^+ pump can increase K_{ATP} channel opening (Haller et al., 2001; Tanner et al., 2011). Further, glycolytic enzymes are associated with membrane proteins (Dhar-Chowdhury et al., 2007; Lu et al., 2001; Mercer and Dunham, 1981; Paul et al., 1979) and have been found to form a complex with K_{ATP} channels (Dhar-Chowdhury et al., 2005; Dubinsky et al., 1998; Hong et al., 2011). Glycolytic inhibition by application of 2DG produces a decrease in cellular and network excitability mediated by K_{ATP} channels and an increase of GABAergic tonic inhibition through neurosteroids (Forte et al., 2016). Even though a direct interaction between BAD and the glycolytic enzyme hexokinase has not been studied, BAD interacts with glucokinase (hexokinase IV) in pancreatic β -cells and hepatocytes (Danial et al., 2008, 2003; Giménez-Cassina et al., 2014), and thus, could be affecting glycolytic ATP production through this interaction. Metabolites other than ATP, such as PIP_2 , also regulate K_{ATP} channels (Li et al., 2017; Martin et al., 2017; Shyng et al., 2000; Shyng and Nichols, 1998), and *Bad* deletion might modify the properties of K_{ATP} channels by altering PIP_2 or through other mechanisms, such as phosphorylation (Béguin et al., 1999).

Conclusion

We have shown that K_{ATP} channels can acutely regulate cellular and network excitability, but whether BAD manipulation itself can affect excitability in an acute manner remains an open question. Inhibitory molecules of BAD's glycolytic role would be valuable to learn the time course by which BAD manipulation exerts its effect on K_{ATP} channels, and thus, seizure protection. Because K_{ATP} channels regulate a wide variety of processes in the brain, targeting the (still unknown) mechanisms that link the BAD-induced change in metabolism to excitability might prove a better pharmacological strategy than targeting neuronal K_{ATP} channels. Mimicking the effect of BAD knockout on fuel preference using small molecules could be a valuable avenue for development of new epilepsy therapies.

Materials and methods

Key resources table

Reagent type (species) or resource	Designation	Source or reference	Identifiers	Additional information
Gene (<i>Mus musculus</i>)	<i>Bad</i>	this paper	HEPDO750_4_D04	for generation of <i>Bad</i> ^{flox/flox} mice
Strain, strain background (<i>Mus musculus</i>)	male or female C57BL/6 mice	Charles River Laboratories		
Genetic reagent (<i>Mus musculus</i>)	male or female homozygous <i>Bad</i> ^{-/-} mice	doi:10.1038/nm1717		
Genetic reagent (<i>Mus musculus</i>)	male or female homozygous <i>Bad</i> ^{-/-} ; <i>Kcnj11</i> ^{-/-} mice	doi:10.1016/j.neuron.2012.03.032		

Continued on next page

Continued

Reagent type (species) or resource	Designation	Source or reference	Identifiers	Additional information
Genetic reagent (<i>Mus musculus</i>)	female heterozygous <i>Dock10-Cre</i> ^{+/-} mice	doi:10.1038/nn.3614		
Genetic reagent (<i>Mus musculus</i>)	male or female homozygous <i>Bad</i> ^{flox/flox} mice	this paper		
Genetic reagent (<i>Mus musculus</i>)	male or female heterozygous <i>Bad</i> ^{flox/flox} , <i>Dock10-Cre</i> ^{+/-} mice	this paper		
Strain, strain background (<i>Adeno-associated virus</i>)	AAV2/8.CAG.BAD.2A.mCherry	BAD-2A-mCherry plasmid packed into AAV8 at Viral Core Boston Children's Hospital		
Strain, strain background (<i>Adeno-associated virus</i>)	AAV2/9.CAG.GCaMP6f	Penn Vector Core	Cat. no. AV-9-PV3081	
Antibody	anti-Bad (rabbit monoclonal)	Abcam	ab32445; RRID:AB_725614	(1:100)
Antibody	anti-Rabbit IgG (goat polyclonal), CF 594	Sigma	SAB4600107	(1:1000)
Other	VECTASHIELD mounting medium with DAPI	Vector Laboratories	H-1200; RRID:AB_2336790	
Software	MATLAB 2016b	Mathworks	RRID:SCR_001622	
Software	Fiji/ImageJ 1.51 s	NIH	RRID:SCR_002285	
Software	Origin 9.1	OriginLab		
Software	Patchmaster v2x43	HEKA		
Software	TILLvisiON 4.0.7.2	Thermo Fisher Scientific		

Reagents

All reagents were purchased from Sigma-Aldrich (St. Louis, MO).

Animals

Brain slice experiments were performed using brains of male and female wild-type mice (C57BL/6; Charles River Laboratories), *Bad*^{-/-} mice (Danial et al., 2008), *Bad*^{+/-}; *Kcnj11*^{-/-} mice (Giménez-Cassina et al., 2012), *Dock10-Cre* mice (Kohara et al., 2014), *Bad*^{flox/flox} mice (see below) or *Bad*^{flox/flox}; *Dock10-Cre* mice. Animals were housed in a barrier facility in individually ventilated cages with ad libitum access to standard chow diet (PicoLab 5058). All experiments were performed in compliance with the NIH Guide for the Care and Use of Laboratory Animals and the Animal Welfare Act. The Harvard Medical Area Standing Committee on Animals approved all procedures involving animals.

Generation of *Bad*^{flox/flox} mice

The ES cell clone bearing the targeting vector of *Bad* gene (HEPD0750_4_D04) was purchased from the European Conditional Mouse Mutagenesis Program, Helmholtz Center Munich, Germany (EUComm ID:92156). The targeted *Bad* allele contained an IRES:LacZ trapping cassette located 5' from a promoter-driven neomycin resistance cassette and inserted upstream of exon 3 flanked by loxP sites (knockout-first-allele design (Skarnes et al., 2011); see also Figure 5A). This allele also contained frt sites to allow simultaneous removal of LacZ and Neo cassettes by Flpase (Flpe)-driven recombination to generate the conditional *Bad*^{flox} allele.

Conditional *Bad*^{flox/flox} mice were generated at the Center for Genome Modification at the University of Connecticut Health, Farmington, CT. Briefly, ES cells (MJ8) were microinjected into blastocysts (BALB/c) to generate chimeric mice that were then crossed to C57BL/6N to generate *BAD*^{flox-*frt*/+} mice. *BAD*^{flox-*frt*/+} mice were then crossed to Flpe mice to remove the lacZ reporter and Neo resistance cassettes. *Bad*^{flox/flox} mice were then mated with *Dock10-Cre* mice (Kohara et al., 2014) to generate *Bad*^{flox/flox}; *Dock10-Cre* mice in which *Bad* is selectively deleted in DGNs.

Viral vectors

Custom-made adeno-associated virus (AAV) vector AAV2/8.CAG.BAD.2A.mCherry was obtained from the Viral Core Facility in Boston Children's Hospital, Boston, MA. AAV2/9.CAG.GCaMP6f (Cat. no. AV-9-PV3081) was obtained from the or the Penn Vector Core, University of Pennsylvania, PA.

GCaMP6f expression in entorhinal-hippocampal area

Mice at postnatal day 1 or 2 were anesthetized by cryoanesthesia. After confirmation of anesthesia, pups were injected intracranially in both hemispheres with 200 nl of either AAV2/8.CAG.BAD.2A.mCherry or AAV2/9.CAG.GCaMP6f. The injection coordinates with respect to lambda were: 0 μm in the anterior-posterior direction, $\pm 2.0 \mu\text{m}$ in the medial-lateral axis and $-2.0 \mu\text{m}$ in the dorsal-ventral direction.

Hippocampal slice preparation for patch-clamp recordings

Juvenile (13 to 19 days old) mice were used for all patch clamp recordings. For BAD reconstitution experiments, mice were injected (at postnatal day 1 or 2) in both hemispheres with 200 nl of AAV2/8.CAG.BAD.2A.mCherry. Mice were anesthetized by isoflurane inhalation and decapitated into ice-cold slicing solution (in mM): 87 NaCl, 2.5 KCl, 1.25 NaH_2PO_4 , 25 NaHCO_3 , 7 MgCl_2 , 0.5 CaCl_2 , 25 D-glucose, 75 sucrose and (osmolality $\sim 340 \text{ mmol/kg}$). The hippocampus was isolated and mounted on a 5% agar cube which was then glued on the stage of a vibrating microtome (Campden Instruments 7000smz, Loughborough, England). Acute hippocampal slices 400 μm thick were cut in the transverse plane. Slices were then incubated at 37°C for 35 min in artificial cerebrospinal fluid (ACSF) containing (in mM): 120 NaCl, 2.5 KCl, 1 NaH_2PO_4 , 26 NaHCO_3 , 1.3 MgCl_2 , 2.5 CaCl_2 , 10 D-glucose ($\sim 300 \text{ mmol/Kg}$, pH 7.4). Additionally, all patch-clamp recording solutions contained 100 μM picrotoxin and 1 mM kynurenic acid to block fast synaptic transmission. These synaptic blockers were directly dissolved into ACSF immediately before experiments. After recovery, slices were stored at room temperature for 0 to 3 hr before use. All solutions were bubbled continuously with 95% O_2 and 5% CO_2 .

Entorhinal-hippocampal slice preparation for epileptiform activity recordings

Juvenile (13 to 19 days old) or adult (60 to 90 days old) mice were injected (at postnatal day 1 or 2) in both hemispheres with 200 nl of AAV2/9.CAG.GCaMP6f. Mice were anesthetized by isoflurane inhalation and then decapitated. The brain was then placed in ice-cold slicing solution (in mM): 87 NaCl, 2.5 KCl, 1.25 NaH_2PO_4 , 25 NaHCO_3 , 7 MgCl_2 , 0.5 CaCl_2 , 25 D-glucose, 75 sucrose and (osmolality $\sim 340 \text{ mmol/kg}$) for juvenile mice or 93 N-Methyl-D-Glucamine, 2.5 KCl, 1.2 NaH_2PO_4 , 30 NaHCO_3 , 10 MgCl_2 , 0.5 CaCl_2 , 25 D-glucose, 20 HEPES, 5 sodium ascorbate, 2 thiourea, 3 sodium pyruvate ($\sim 320 \text{ mmol/Kg}$; pH 7.4 adjusted with HCl) for adult mice (Ting et al., 2014). Acute slices 450 μm thick were cut in the transverse plane using a vibrating microtome (Campden Instruments 7000smz, Loughborough, England). Slices were allowed to recover at 37°C for 35 min in artificial cerebrospinal fluid (ACSF) containing (in mM): 120 NaCl, 2.5 KCl, 1 NaH_2PO_4 , 26 NaHCO_3 , 1 MgCl_2 , 2 CaCl_2 , 10 D-glucose ($\sim 300 \text{ mmol/Kg}$, pH 7.4). After recovery, slices were stored at room temperature for 0 to 3 hr before use. All solutions were bubbled continuously with 95% O_2 and 5% CO_2 . Picrotoxin was prepared daily before recordings from 50 or 500 mM stock solutions in DMSO and diluted to 2.5 or 50 μM , respectively, in recording solution. The concentration of DMSO as a vehicle control in ACSF was adjusted accordingly to 0.005% or 0.01%.

Patch-clamp recordings

Whole-cell and perforated-patch recordings from individual dentate granule neurons (DGNs) identified under infrared differential interference contrast (IR-DIC) visual guidance were made in voltage-clamp mode following establishment of high-resistance (multi-G Ω) seals. For BAD reconstitution experiments, mCherry was excited at 580 nm using a Xenon lamp and monochromator (Polychrome IV, Thermo Fisher Scientific). Images were collected with a CCD camera (IMAGO-QE, Thermo Fisher Scientific) and TILLvisION software (Thermo Fisher Scientific). Electrophysiological data were collected with a HEKA EPC 10 patch-clamp amplifier (HEKA, Holliston, MA). Currents were filtered at 1 kHz and sampled at 10 kHz. Patchmaster v2x43 software (HEKA, Holliston, MA) was used for

amplifier control and data acquisition. Patch pipettes were pulled from borosilicate glass (VWR Scientific) using a Sutter Instruments P-97 puller. Pipette tips were fire polished to resistances of 2–3 M Ω when filled with recording solutions. During recording, ACSF was delivered to the recording bath using a peristaltic pump at a flow rate of 1 ml/min at room temperature.

For whole-cell recordings the pipette solution contained (in mM): 140 KMeS, 10 NaCl, 10 HEPES, 1 MgCl₂, and 0.1 EGTA (osmolality ~295 mmol/kg; pH 7.4), supplemented with 0.3 mM NaGTP and either 0.3 or 4 mM MgATP. A voltage ramp protocol was used to measure input resistance and slope conductance: from the –70 mV holding potential followed two 100 ms steps first to –100 mV then to –120 mV before initiation of a 1 s ramp from –120 to –60 mV. The prepulses were used to calculate the cell's input resistance. Voltage ramps were applied every 10 s and fitted with a straight line from –120 to –90 mV to provide a running assessment of whole-cell slope conductance.

For perforated-patch recordings, the pipette tip was filled with whole-cell pipette solution and backfilled with the same solution with amphotericin B (200 μ g/ml) and Alexa Fluor 488 (10 μ M; Invitrogen) added. This solution was vortexed immediately before each neuron was patched. Giga-ohm seals were achieved before amphotericin B arrived at the pipette tip, as assessed by monitoring Alexa Fluor 488 fluorescence. The access resistance was then continuously monitored and recordings started when the access resistance was <100 M Ω . Experiments where access resistance changed >20% during the experiment or seals that took longer than 15 min to perforate were discarded. The integrity of perforated-patch recordings was judged by monitoring Alexa Fluor 488 fluorescence, and recordings where dye entered the cell were discarded. To limit recordings to a population of neurons in a homogeneous stage of DGN maturation, perforated-patch experiments were performed in DGNs with membrane capacitance of 30–40 pF. Amphotericin B was stored at –20°C in 20 mg/ml stock solutions in DMSO for one week maximum. Glibenclamide (200 nM) was diluted in ACSF from a 0.5 mM stock solution in DMSO. DMSO as a vehicle control was added to ACSF at 0.02%. Glibenclamide was applied for 10 min before recording its presence. The current clamp protocol consisted on injecting sufficient current (<30 pA) to maintain the membrane potential at –70 mV. A series of 1 s current pulses (10 s interval between pulses) were applied from 50 to 200 pA in 50 pA steps. Experiments were performed with experimenter blind to genotype.

Patch-clamp data analysis

Data and statistical analysis were performed with Patchmaster v2x43 (HEKA, Holliston, MA) and Origin 9.1 (OriginLab, Northampton, MA, USA). The number of independent experiments (n) corresponds to the number of patched cells from different hippocampal slices. In all cases, each experimental condition was tested in slices from at least three different animals.

Epileptiform activity recordings

In our efforts to study seizure-like activity we devised a non-electrophysiological in vitro paradigm to monitor SLEs using the fluorescent calcium sensor GCaMP6f. Epileptiform activity in the EC-HC region has been extensively studied using electrophysiological methods in acute slices (**Avoli and Jefferys, 2016**). A plethora of methods to elicit epileptiform activity in EC-HC slices have been utilized, including inhibition of potassium channels with 4-aminopyridine (**Brückner and Heinemann, 2000; Buckle and Haas, 1982; Galvan et al., 1982; Michelson and Wong, 1991; Rutecki et al., 1987; Voskuyl and Albus, 1985; Watts and Jefferys, 1993**), disinhibiting glutamate receptors by lowering the extracellular magnesium concentration (**Bragdon et al., 1992; Dreier and Heinemann, 1991; Khosravani et al., 2005; Mody et al., 1987; Walther et al., 1986; Whittington et al., 1995; Zhang et al., 1995**), or inhibition of GABA_A receptors with picrotoxin (**Hablitz, 1984; Hablitz and Heinemann, 1989; Lee and Hablitz, 1989; Miles et al., 1984**). Compared to in vivo experiments, these seizure-like activity paradigms have several advantages, such as straightforward access to perfuse pharmacological agents and higher experimental throughput. We chose to study epileptiform activity by extracellular picrotoxin application due to the reliability of triggering SLEs slice to slice (SLEs were observed in all slices treated with picrotoxin), short latency of SLE induction and robustness of epileptiform bursts.

We sought to further increase throughput by avoiding placing electrodes in the preparation and increasing the spatial coverage of the area being monitored to the whole EC-HC region. The majority of the studies of epileptiform activity in brain slices have been performed using single-electrode

extracellular recordings, planar multielectrode arrays (Hongo et al., 2015; Simeone et al., 2014, 2013), or tetrode wire recordings (Lévesque et al., 2016). These methods, while having high temporal resolution, are limited to the number of electrodes that can be placed in the preparation, limiting the spatial coverage. To circumvent this constraint, in vitro epileptiform activity has also been investigated by optical methods including the monitoring of intrinsic optical signals (Aitken et al., 1999; Borbély et al., 2014; D'Arcangelo et al., 2001; Weissinger et al., 2000) or fluorescence of voltage-sensitive dyes (Bikson et al., 2004; Carlson and Coulter, 2008; Chang et al., 2007; Hazra et al., 2012; Sinha and Saggau, 2001). These optical methods allow for examination of seizure-like activity over a wide tissue area, however, their signal-to-noise ratio is poor and the dynamic range is very limited (a few percent), thus requiring significant signal averaging and decreasing even further temporal resolution. We expressed GCaMP6f, a fluorescent calcium sensor that has superior signal-to-noise ratio (typically a maximum of ~50% $\Delta F/F$ in our experiments) and with temporal dynamics adequate to discern picrotoxin-elicited SLEs (Chen et al., 2013). To monitor epifluorescence in the entirety of the EC-HC network we used a low magnification (4X) objective which makes this technique straightforward.

It is technically challenging to sufficiently oxygenate brain slices to preserve network dynamics in submerged conditions (Hájos et al., 2009; Hájos and Mody, 2009; Huchzermeyer et al., 2008). In a typical submerged chamber, the slices are in contact with the bath solution only on one side, thus, to achieve sufficient oxygenation, very high perfusion rates (>15 mL/min) are necessary to preserve network activity. To monitor epileptiform activity through GCaMP6f epifluorescence, we used a dual perfusion chamber, where acute slices are sitting in a grate in contact with oxygenated solution on both sides (Hájos et al., 2009; Hájos and Mody, 2009; Lutas et al., 2014). The dual perfusion chamber permits maintaining sufficiently high oxygenation for the generation of SLEs while also greatly facilitating imaging with an unsubmerged low-power objective to visualize the whole EC-HC area. In part this is due to perfusion rates (5 mL/min) that create a suitably undisturbed surface. This new in vitro setting greatly facilitates the study of epileptiform activity and can be easily modified to monitor other fluorescent sensors.

We recorded fluorescence intensity recordings in a dual-perfusion chamber where the slices are in contact with oxygenated ACSF on both sides continuously at a rate of 5 ml/min (2.5 ml/min/line) (Hájos and Mody, 2009). A slice anchor (Warner Instruments, Hamden, CT) was placed on each slice to prevent its movement during the experiment. Bath temperature was maintained at 34°C using one inline heater (Warner Instruments, Hamden, CT) per perfusion line. Solutions were kept in a water bath (VWR) at 37°C during the experiments to prevent out-gassing while being bubbled continuously with 95% O₂ and 5% CO₂. Slices were visualized with an Olympus BX51WI upright microscope using a 4X (NA 0.1 or 0.13) objective. GCaMP6f was excited at 485 nm using a Xenon lamp and monochromator (Polychrome IV, Thermo Fisher Scientific). Images were collected with a CCD camera (IMAGO-QE, Thermo Fisher Scientific) at a rate of 10 frames per second with TILLvision software (Thermo Fisher Scientific).

Regions of interest were drawn with ImageJ (NIH) to analyze GCaMP6f fluorescence intensity changes ($\Delta F/F$) in the entorhinal cortex or hippocampus. Subsequent analysis was performed using laboratory-made software in MATLAB (Mathworks, Natick, MA). Epileptiform activity $\Delta F/F$ time courses were filtered to account for baseline drift of the signal. Then, a threshold was set according to each trace signal-to-noise ratio and $\Delta F/F$ values above threshold were defined as seizure-like events (SLEs). Fraction of time spent in SLEs as a function of time was plotted in 5 min bins.

Immunohistochemistry

Juvenile mice (16 to 25 days old) were anesthetized with 100 mg Ketamine/10 mg Xylazine i.p. per kg. Anesthesia was confirmed prior to intracardiac perfusion with PBS 1X followed by 4% paraformaldehyde (PFA) in PBS pH 7.4. Brains were immediately extracted, fixed overnight in 4% PFA at 4°C and, cryoprotected in 30% sucrose in PBS for 48 hr at 4°C, embedded in Tissue-TeK OCT (Sakura) and frozen on dry ice. Coronal or horizontal tissue sections (30 μ m thick) were cut with cryostat.

Primary and secondary antibodies were prepared in blocking solution (PBS with 0.1% Triton, 10% FBS and 3 mg/ml BSA). Brain sections were treated with blocking solution for 3 hr at room temperature, incubated with BAD primary antibody (1:100, Abcam ab32445) overnight at 4°C and with secondary anti-rabbit (1:1000, Sigma SAB4600107) for 1 hr at room temperature. Tissue sections were

mounted with Vectashield Mounting Medium with DAPI (Vector Laboratories). Sections were imaged using an Olympus VS120 microscope and the secondary antibody's CF 594 fluorescence was excited with 594 nm light. For all representative images displayed in the figures, experiments were successfully repeated three or more times.

Data and statistical analysis

The number of independent experiments (n) is indicated in each figure. For calcium imaging data, number of animals (N) is also reported. For electrophysiology experiments, sample sizes were based on previous studies (*Giménez-Cassina et al., 2012*); for calcium imaging experiments, sample sizes and power analysis were not determined in advance due to lack of knowledge of variability and likely effect sizes. In boxplots, central line indicates the median; bottom and top edges of the box indicate the 25th and 75th percentiles, respectively; whiskers extend to all data points not considered outliers; open symbols indicate outliers; and shaded area indicates 95% confidence intervals. Other summary data are presented as mean \pm SEM, as indicated. Data were normally distributed and statistical significance was determined using two-tailed Student's t test or 1-way ANOVA with Bonferroni *post hoc* test as indicated. Statistical analyses were performed using MATLAB (Mathworks, Natick, MA) or Origin 9.1 (OriginLab, Northampton, MA, USA).

Acknowledgements

We thank Sofia M. Ribeiro, Binsen Li and Hannah Zucker for assistance in the generation of AAV vectors, and members of the Danial and Yellen laboratories for critical reading of this manuscript and valuable discussions. We also thank Dr. Susumu Tonegawa for providing the *Dock10-Cre* transgenic mice; the Viral Core of Boston Children's Hospital and the U Penn Vector Core for packaging of AAVs; the GENIE project of HHMI Janelia Research Campus, Dr. Loren Looger and Dr. Douglas Kim for the GCaMP6f sensor. MCFA was supported by an EMBO long-term postdoctoral fellowship (473-2016). This work was supported by NIH grants R01 NS083844 (to NND and GY) and R01 NS055031 (to GY). This work was also assisted by core facilities supported by NIH grants P30 NS072030 (Harvard Medical School Neurobiology Imaging Facility) and P30 EY012196 (Harvard Medical School Neurobiology Machine Shop).

Additional information

Funding

Funder	Grant reference number	Author
National Institutes of Health	R01 NS083844	Nika Danial Gary Yellen
National Institutes of Health	R01 NS055031	Gary Yellen
European Molecular Biology Organization	473-2016	María Carmen Fernández-Agüera
National Institutes of Health	DP1 EB016985	Gary Yellen

The funders had no role in study design, data collection and interpretation, or the decision to submit the work for publication.

Author contributions

Juan Ramón Martínez-François, Conceptualization, Investigation, Methodology, Writing—original draft, Writing—review and editing; María Carmen Fernández-Agüera, Investigation, Methodology, Writing—review and editing; Nidhi Nathwani, Veronica L Burnham, Investigation, Writing—review and editing; Carolina Lahmann, Supervision, Investigation, Writing—review and editing; Nika N Danial, Resources, Supervision, Funding acquisition, Writing—review and editing; Gary Yellen, Conceptualization, Supervision, Funding acquisition, Writing—review and editing

Author ORCIDs

Juan Ramón Martínez-François  <http://orcid.org/0000-0002-1035-2574>

María Carmen Fernández-Agüera  <http://orcid.org/0000-0002-0769-213X>

Gary Yellen  <http://orcid.org/0000-0003-4228-7866>

Ethics

Animal experimentation: All experiments were performed in compliance with the NIH Guide for the Care and Use of Laboratory Animals and the Animal Welfare Act. The Harvard Medical Area Standing Committee on Animals approved all procedures involving animals (protocol #03506, assurance A3431-01).

Decision letter and Author response

Decision letter <https://doi.org/10.7554/eLife.32721.017>

Author response <https://doi.org/10.7554/eLife.32721.018>

Additional files**Supplementary files**

- Transparent reporting form

DOI: <https://doi.org/10.7554/eLife.32721.015>

References

- Aguilar-Bryan L**, Clement JP, Gonzalez G, Kunjilwar K, Babenko A, Bryan J. 1998. Toward understanding the assembly and structure of K_{ATP} channels. *Physiological Reviews* **78**:227–245. DOI: <https://doi.org/10.1152/physrev.1998.78.1.227>, PMID: 9457174
- Aitken PG**, Fayuk D, Somjen GG, Turner DA. 1999. Use of intrinsic optical signals to monitor physiological changes in brain tissue slices. *Methods* **18**:91–103. DOI: <https://doi.org/10.1006/meth.1999.0762>, PMID: 10356339
- Allen TG**, Brown DA. 2004. Modulation of the excitability of cholinergic basal forebrain neurones by K_{ATP} channels. *The Journal of Physiology* **554**:353–370. DOI: <https://doi.org/10.1113/jphysiol.2003.055889>, PMID: 14578474
- Andersen P**, Holmqvist B, Voorhoeve PE. 1966. Entorhinal activation of dentate granule cells. *Acta Physiologica Scandinavica* **66**:448–460. DOI: <https://doi.org/10.1111/j.1748-1716.1966.tb03223.x>, PMID: 5927271
- Ang CW**, Carlson GC, Coulter DA. 2006. Massive and specific dysregulation of direct cortical input to the hippocampus in temporal lobe epilepsy. *Journal of Neuroscience* **26**:11850–11856. DOI: <https://doi.org/10.1523/JNEUROSCI.2354-06.2006>, PMID: 17108158
- Appleton DB**, DeVivo DC. 1974. An animal model for the ketogenic diet. *Epilepsia* **15**:211–227. DOI: <https://doi.org/10.1111/j.1528-1157.1974.tb04943.x>, PMID: 4525180
- Ashford ML**, Boden PR, Treherne JM. 1990. Glucose-induced excitation of hypothalamic neurones is mediated by ATP-sensitive K^+ channels. *Pflügers Archiv European Journal of Physiology* **415**:479–483. DOI: <https://doi.org/10.1007/BF00373626>, PMID: 2315006
- Avoli M**, Jefferys JG. 2016. Models of drug-induced epileptiform synchronization *in vitro*. *Journal of Neuroscience Methods* **260**:26–32. DOI: <https://doi.org/10.1016/j.jneumeth.2015.10.006>, PMID: 26484784
- Barbarosie M**, Avoli M. 1997. CA3-driven hippocampal-entorhinal loop controls rather than sustains *in vitro* limbic seizures. *Journal of Neuroscience* **17**:9308–9314. PMID: 9364076
- Barbarosie M**, Louvel J, Kurcewicz I, Avoli M. 2000. CA3-released entorhinal seizures disclose dentate gyrus epileptogenicity and unmask a temporoammonic pathway. *Journal of Neurophysiology* **83**:1115–1124. DOI: <https://doi.org/10.1152/jn.2000.83.3.1115>, PMID: 10712442
- Behr J**, Lyson KJ, Mody I. 1998. Enhanced propagation of epileptiform activity through the kindled dentate gyrus. *Journal of Neurophysiology* **79**:1726–1732. DOI: <https://doi.org/10.1152/jn.1998.79.4.1726>, PMID: 9535942
- Ben-Ari Y**, Khalilov I, Kahle KT, Cherubini E. 2012. The GABA excitatory/inhibitory shift in brain maturation and neurological disorders. *The Neuroscientist* **18**:467–486. DOI: <https://doi.org/10.1177/1073858412438697>, PMID: 22547529
- Bikson M**, Inoue M, Akiyama H, Deans JK, Fox JE, Miyakawa H, Jefferys JG. 2004. Effects of uniform extracellular DC electric fields on excitability in rat hippocampal slices *in vitro*. *The Journal of Physiology* **557**:175–190. DOI: <https://doi.org/10.1113/jphysiol.2003.055772>, PMID: 14978199
- Borbély S**, Körössy C, Somogyvári Z, Világi I. 2014. *In vitro* intrinsic optical imaging can be used for source determination in cortical slices. *European Journal of Neuroscience* **39**:72–82. DOI: <https://doi.org/10.1111/ejn.12384>, PMID: 24118173

- Bough KJ**, Wetherington J, Hassel B, Pare JF, Gawryluk JW, Greene JG, Shaw R, Smith Y, Geiger JD, Dingledine RJ. 2006. Mitochondrial biogenesis in the anticonvulsant mechanism of the ketogenic diet. *Annals of Neurology* **60**:223–235. DOI: <https://doi.org/10.1002/ana.20899>, PMID: 16807920
- Bough KJ**, Rho JM. 2007. Anticonvulsant mechanisms of the ketogenic diet. *Epilepsia* **48**:43–58. DOI: <https://doi.org/10.1111/j.1528-1167.2007.00915.x>, PMID: 17241207
- Bragdon AC**, Kojima H, Wilson WA. 1992. Suppression of interictal bursting in hippocampus unleashes seizures in entorhinal cortex: a proepileptic effect of lowering $[K^+]_o$ and raising $[Ca^{2+}]_o$. *Brain Research* **590**:128–135. DOI: [https://doi.org/10.1016/0006-8993\(92\)91088-V](https://doi.org/10.1016/0006-8993(92)91088-V), PMID: 1422827
- Brückner C**, Heinemann U. 2000. Effects of standard anticonvulsant drugs on different patterns of epileptiform discharges induced by 4-aminopyridine in combined entorhinal cortex-hippocampal slices. *Brain Research* **859**:15–20. DOI: [https://doi.org/10.1016/S0006-8993\(99\)02348-3](https://doi.org/10.1016/S0006-8993(99)02348-3), PMID: 10720610
- Buckle PJ**, Haas HL. 1982. Enhancement of synaptic transmission by 4-aminopyridine in hippocampal slices of the rat. *The Journal of Physiology* **326**:109–122. DOI: <https://doi.org/10.1113/jphysiol.1982.sp014180>, PMID: 6286946
- Béguin P**, Nagashima K, Nishimura M, Gonoi T, Seino S. 1999. PKA-mediated phosphorylation of the human K_{ATP} channel: separate roles of Kir6.2 and SUR1 subunit phosphorylation. *The EMBO Journal* **18**:4722–4732. DOI: <https://doi.org/10.1093/emboj/18.17.4722>, PMID: 10469651
- Carlson GC**, Coulter DA. 2008. *In vitro* functional imaging in brain slices using fast voltage-sensitive dye imaging combined with whole-cell patch recording. *Nature Protocols* **3**:249–255. DOI: <https://doi.org/10.1038/nprot.2007.539>, PMID: 18274527
- Chang PY**, Taylor PE, Jackson MB. 2007. Voltage imaging reveals the CA1 region at the CA2 border as a focus for epileptiform discharges and long-term potentiation in hippocampal slices. *Journal of Neurophysiology* **98**:1309–1322. DOI: <https://doi.org/10.1152/jn.00532.2007>, PMID: 17615129
- Chen TW**, Wardill TJ, Sun Y, Pulver SR, Renninger SL, Baohan A, Schreier ER, Kerr RA, Orger MB, Jayaraman V, Looger LL, Svoboda K, Kim DS. 2013. Ultrasensitive fluorescent proteins for imaging neuronal activity. *Nature* **499**:295–300. DOI: <https://doi.org/10.1038/nature12354>, PMID: 23868258
- D’Arcangelo G**, Tancredi V, Avoli M. 2001. Intrinsic optical signals and electrographic seizures in the rat limbic system. *Neurobiology of Disease* **8**:993–1005. DOI: <https://doi.org/10.1006/nbdi.2001.0445>, PMID: 11741395
- Danial NN**, Gramm CF, Scorrano L, Zhang CY, Krauss S, Ranger AM, Datta SR, Greenberg ME, Licklider LJ, Lowell BB, Gygi SP, Korsmeyer SJ. 2003. BAD and glucokinase reside in a mitochondrial complex that integrates glycolysis and apoptosis. *Nature* **424**:952–956. DOI: <https://doi.org/10.1038/nature01825>, PMID: 12931191
- Danial NN**, Walensky LD, Zhang CY, Choi CS, Fisher JK, Molina AJ, Datta SR, Pitter KL, Bird GH, Wikstrom JD, Deeney JT, Robertson K, Morash J, Kulkarni A, Neschen S, Kim S, Greenberg ME, Corkey BE, Shirihai OS, Shulman GI, et al. 2008. Dual role of proapoptotic BAD in insulin secretion and beta cell survival. *Nature Medicine* **14**:144–153. DOI: <https://doi.org/10.1038/nm1717>, PMID: 18223655
- DeVivo DC**, Leckie MP, Ferrendelli JS, McDougal DB. 1978. Chronic ketosis and cerebral metabolism. *Annals of Neurology* **3**:331–337. DOI: <https://doi.org/10.1002/ana.410030410>, PMID: 666275
- Dengler CG**, Coulter DA. 2016. Normal and epilepsy-associated pathologic function of the dentate gyrus. *Progress in Brain Research* **226**:155–178. DOI: <https://doi.org/10.1016/bs.pbr.2016.04.005>, PMID: 27323942
- Dhar-Chowdhury P**, Harrell MD, Han SY, Jankowska D, Parachuru L, Morrissey A, Srivastava S, Liu W, Malester B, Yoshida H, Coetzee WA. 2005. The glycolytic enzymes, glyceraldehyde-3-phosphate dehydrogenase, triose-phosphate isomerase, and pyruvate kinase are components of the K_{ATP} channel macromolecular complex and regulate its function. *Journal of Biological Chemistry* **280**:38464–38470. DOI: <https://doi.org/10.1074/jbc.M508744200>, PMID: 16170200
- Dhar-Chowdhury P**, Malester B, Rajacic P, Coetzee WA. 2007. The regulation of ion channels and transporters by glycolytically derived ATP. *Cellular and Molecular Life Sciences* **64**:3069–3083. DOI: <https://doi.org/10.1007/s00018-007-7332-3>, PMID: 17882378
- Dreier JP**, Heinemann U. 1991. Regional and time dependent variations of low Mg^{2+} induced epileptiform activity in rat temporal cortex slices. *Experimental Brain Research* **87**:581–596. DOI: <https://doi.org/10.1007/BF00227083>, PMID: 1783028
- Dubinsky WP**, Mayorga-Wark O, Schultz SG. 1998. Colocalization of glycolytic enzyme activity and K_{ATP} channels in basolateral membrane of Necturus enterocytes. *American Journal of Physiology-Cell Physiology* **275**:C1653–C1659. DOI: <https://doi.org/10.1152/ajpcell.1998.275.6.C1653>, PMID: 9843727
- Dunn-Meynell AA**, Rawson NE, Levin BE. 1998. Distribution and phenotype of neurons containing the ATP-sensitive K^+ channel in rat brain. *Brain Research* **814**:41–54. DOI: [https://doi.org/10.1016/S0006-8993\(98\)00956-1](https://doi.org/10.1016/S0006-8993(98)00956-1), PMID: 9838037
- Engel T**, Hatazaki S, Tanaka K, Prehn JH, Henshall DC. 2010. Deletion of Puma protects hippocampal neurons in a model of severe status epilepticus. *Neuroscience* **168**:443–450. DOI: <https://doi.org/10.1016/j.neuroscience.2010.03.057>, PMID: 20362645
- Engel T**, Plesnila N, Prehn JH, Henshall DC. 2011. *In vivo* contributions of BH3-only proteins to neuronal death following seizures, ischemia, and traumatic brain injury. *Journal of Cerebral Blood Flow & Metabolism* **31**:1196–1210. DOI: <https://doi.org/10.1038/jcbfm.2011.26>, PMID: 21364604
- Espósito MS**, Piatti VC, Laplagne DA, Morgenstern NA, Ferrari CC, Pitossi FJ, Schinder AF. 2005. Neuronal differentiation in the adult hippocampus recapitulates embryonic development. *Journal of Neuroscience* **25**:10074–10086. DOI: <https://doi.org/10.1523/JNEUROSCI.3114-05.2005>, PMID: 16267214

- Foley J, Burnham V, Tedoldi M, Danial NN, Yellen G. 2018. BAD knockout provides metabolic seizure resistance in a genetic model of epilepsy with sudden unexplained death in epilepsy. *Epilepsia* **59**:e1–e4. DOI: <https://doi.org/10.1111/epi.13960>, PMID: 29171006
- Forté N, Medrihan L, Cappetti B, Baldelli P, Benfenati F. 2016. 2-Deoxy-d-glucose enhances tonic inhibition through the neurosteroid-mediated activation of extrasynaptic GABAA receptors. *Epilepsia* **57**:1987–2000. DOI: <https://doi.org/10.1111/epi.13578>, PMID: 27735054
- Galvan M, Grafe P, ten Bruggencate G. 1982. Convulsant actions of 4-aminopyridine on the guinea-pig olfactory cortex slice. *Brain Research* **241**:75–86. DOI: [https://doi.org/10.1016/0006-8993\(82\)91230-6](https://doi.org/10.1016/0006-8993(82)91230-6), PMID: 7104708
- Garriga-Canut M, Schoenike B, Qazi R, Bergendahl K, Daley TJ, Pfender RM, Morrison JF, Ockuly J, Stafstrom C, Sutula T, Roopra A. 2006. 2-Deoxy-D-glucose reduces epilepsy progression by NRSF-CtBP-dependent metabolic regulation of chromatin structure. *Nature Neuroscience* **9**:1382–1387. DOI: <https://doi.org/10.1038/nn1791>, PMID: 17041593
- Giménez-Cassina A, Martínez-François JR, Fisher JK, Szlyk B, Polak K, Wiwczar J, Tanner GR, Lutas A, Yellen G, Danial NN. 2012. BAD-dependent regulation of fuel metabolism and K_{ATP} channel activity confers resistance to epileptic seizures. *Neuron* **74**:719–730. DOI: <https://doi.org/10.1016/j.neuron.2012.03.032>, PMID: 22632729
- Giménez-Cassina A, Garcia-Haro L, Choi CS, Osundiji MA, Lane EA, Huang H, Yildirim MA, Szlyk B, Fisher JK, Polak K, Patton E, Wiwczar J, Godes M, Lee DH, Robertson K, Kim S, Kulkarni A, Distefano A, Samuel V, Cline G, et al. 2014. Regulation of hepatic energy metabolism and gluconeogenesis by BAD. *Cell Metabolism* **19**:272–284. DOI: <https://doi.org/10.1016/j.cmet.2013.12.001>, PMID: 24506868
- Giménez-Cassina A, Danial NN. 2015. Regulation of mitochondrial nutrient and energy metabolism by BCL-2 family proteins. *Trends in Endocrinology & Metabolism* **26**:165–175. DOI: <https://doi.org/10.1016/j.tem.2015.02.004>, PMID: 25748272
- Hablitz JJ. 1984. Picrotoxin-induced epileptiform activity in hippocampus: role of endogenous versus synaptic factors. *Journal of Neurophysiology* **51**:1011–1027. DOI: <https://doi.org/10.1152/jn.1984.51.5.1011>, PMID: 6327932
- Hablitz JJ, Heinemann U. 1989. Alterations in the microenvironment during spreading depression associated with epileptiform activity in the immature neocortex. *Developmental Brain Research* **46**:243–252. DOI: [https://doi.org/10.1016/0165-3806\(89\)90288-5](https://doi.org/10.1016/0165-3806(89)90288-5), PMID: 2720957
- Haller M, Mironov SL, Karschin A, Richter DW. 2001. Dynamic activation of K_{ATP} channels in rhythmically active neurons. *The Journal of Physiology* **537**:69–81. DOI: <https://doi.org/10.1111/j.1469-7793.2001.0069k.x>, PMID: 11711562
- Hartman AL, Gasior M, Vining EP, Rogawski MA. 2007. The neuropharmacology of the ketogenic diet. *Pediatric Neurology* **36**:281–292. DOI: <https://doi.org/10.1016/j.pediatrneurol.2007.02.008>, PMID: 17509459
- Hazra A, Rosenbaum R, Bodmann B, Cao S, Josić K, Žiburkus J. 2012. β -Adrenergic modulation of spontaneous spatiotemporal activity patterns and synchrony in hyperexcitable hippocampal circuits. *Journal of Neurophysiology* **108**:658–671. DOI: <https://doi.org/10.1152/jn.00708.2011>, PMID: 22496530
- Heinemann U, Beck H, Dreier JP, Ficker E, Stabel J, Zhang CL. 1992. The dentate gyrus as a regulated gate for the propagation of epileptiform activity. *Epilepsy Research. Supplement* **7**:273–280. PMID: 1334666
- Hollrigel GS, Ross ST, Soltesz I. 1998. Temporal patterns and depolarizing actions of spontaneous GABA_A receptor activation in granule cells of the early postnatal dentate gyrus. *Journal of Neurophysiology* **80**:2340–2351. DOI: <https://doi.org/10.1152/jn.1998.80.5.2340>, PMID: 9819247
- Holmes GL, Ben-Ari Y. 2001. The neurobiology and consequences of epilepsy in the developing brain. *Pediatric Research* **49**:320–325. DOI: <https://doi.org/10.1203/00006450-200103000-00004>, PMID: 11228256
- Hong M, Kefaloyianni E, Bao L, Malester B, Delaroché D, Neubert TA, Coetzee WA. 2011. Cardiac ATP-sensitive K^+ channel associates with the glycolytic enzyme complex. *The FASEB Journal* **25**:2456–2467. DOI: <https://doi.org/10.1096/fj.10-176669>, PMID: 21482559
- Hongo Y, Takasu K, Ikegaya Y, Hasegawa M, Sakaguchi G, Ogawa K. 2015. Heterogeneous effects of antiepileptic drugs in an *in vitro* epilepsy model—a functional multineuron calcium imaging study. *European Journal of Neuroscience* **42**:1818–1829. DOI: <https://doi.org/10.1111/ejn.12945>, PMID: 25967117
- Hsu D. 2007. The dentate gyrus as a filter or gate: a look back and a look ahead. *Progress in Brain Research* **163**:601–613. DOI: [https://doi.org/10.1016/S0079-6123\(07\)63032-5](https://doi.org/10.1016/S0079-6123(07)63032-5), PMID: 17765740
- Huchzermeyer C, Albus K, Gabriel HJ, Otáhal J, Taubenberger N, Heinemann U, Kovács R, Kann O. 2008. Gamma oscillations and spontaneous network activity in the hippocampus are highly sensitive to decreases in pO_2 and concomitant changes in mitochondrial redox state. *Journal of Neuroscience* **28**:1153–1162. DOI: <https://doi.org/10.1523/JNEUROSCI.4105-07.2008>, PMID: 18234893
- Huttenlocher PR. 1976. Ketoneemia and seizures: metabolic and anticonvulsant effects of two ketogenic diets in childhood epilepsy. *Pediatric Research* **10**:536–540. DOI: <https://doi.org/10.1203/00006450-197605000-00006>, PMID: 934725
- Hájos N, Ellender TJ, Zemankovics R, Mann EO, Exley R, Cragg SJ, Freund TF, Paulsen O. 2009. Maintaining network activity in submerged hippocampal slices: importance of oxygen supply. *European Journal of Neuroscience* **29**:319–327. DOI: <https://doi.org/10.1111/j.1460-9568.2008.06577.x>, PMID: 19200237
- Hájos N, Mody I. 2009. Establishing a physiological environment for visualized *in vitro* brain slice recordings by increasing oxygen supply and modifying aCSF content. *Journal of Neuroscience Methods* **183**:107–113. DOI: <https://doi.org/10.1016/j.jneumeth.2009.06.005>, PMID: 19524611
- Jiao S, Li Z. 2011. Nonapoptotic function of BAD and BAX in long-term depression of synaptic transmission. *Neuron* **70**:758–772. DOI: <https://doi.org/10.1016/j.neuron.2011.04.004>, PMID: 21609830

- Juge N**, Gray JA, Omote H, Miyaji T, Inoue T, Hara C, Uneyama H, Edwards RH, Nicoll RA, Moriyama Y. 2010. Metabolic control of vesicular glutamate transport and release. *Neuron* **68**:99–112. DOI: <https://doi.org/10.1016/j.neuron.2010.09.002>, PMID: 20920794
- Karschin C**, Ecke C, Ashcroft FM, Karschin A. 1997. Overlapping distribution of K_{ATP} channel-forming Kir6.2 subunit and the sulfonylurea receptor SUR1 in rodent brain. *FEBS Letters* **401**:59–64. DOI: [https://doi.org/10.1016/S0014-5793\(96\)01438-X](https://doi.org/10.1016/S0014-5793(96)01438-X), PMID: 9003806
- Khosravani H**, Pinnegar CR, Mitchell JR, Bardakjian BL, Federico P, Carlen PL. 2005. Increased high-frequency oscillations precede in vitro low-Mg seizures. *Epilepsia* **46**:1188–1197. DOI: <https://doi.org/10.1111/j.1528-1167.2005.65604.x>, PMID: 16060927
- Kohara K**, Pignatelli M, Rivest AJ, Jung HY, Kitamura T, Suh J, Frank D, Kajikawa K, Mise N, Obata Y, Wickersham IR, Tonegawa S. 2014. Cell type-specific genetic and optogenetic tools reveal hippocampal CA2 circuits. *Nature Neuroscience* **17**:269–279. DOI: <https://doi.org/10.1038/nn.3614>, PMID: 24336151
- Krook-Magnuson E**, Armstrong C, Oijala M, Soltesz I. 2013. On-demand optogenetic control of spontaneous seizures in temporal lobe epilepsy. *Nature Communications* **4**:1376. DOI: <https://doi.org/10.1038/ncomms2376>, PMID: 23340416
- Krook-Magnuson E**, Armstrong C, Bui A, Lew S, Oijala M, Soltesz I. 2015. In vivo evaluation of the dentate gate theory in epilepsy. *The Journal of Physiology* **593**:2379–2388. DOI: <https://doi.org/10.1113/JP270056>, PMID: 25752305
- Lee WL**, Hablitz JJ. 1989. Involvement of non-NMDA receptors in picrotoxin-induced epileptiform activity in the hippocampus. *Neuroscience Letters* **107**:129–134. DOI: [https://doi.org/10.1016/0304-3940\(89\)90804-5](https://doi.org/10.1016/0304-3940(89)90804-5), PMID: 2575723
- Levin BE**. 2002. Metabolic sensors: viewing glucosensing neurons from a broader perspective. *Physiology & Behavior* **76**:397–401. DOI: [https://doi.org/10.1016/S0031-9384\(02\)00763-1](https://doi.org/10.1016/S0031-9384(02)00763-1), PMID: 12117576
- Li N**, Wu JX, Ding D, Cheng J, Gao N, Chen L. 2017. Structure of a pancreatic ATP-sensitive potassium channel. *Cell* **168**:101–110. DOI: <https://doi.org/10.1016/j.cell.2016.12.028>, PMID: 28086082
- Liss B**, Roeper J. 2001. Molecular physiology of neuronal K-ATP channels. *Molecular Membrane Biology* **18**:117–127. DOI: <https://doi.org/10.1080/09687680110047373>, PMID: 11463204
- Liu YB**, Lio PA, Pasternak JF, Trommer BL. 1996. Developmental changes in membrane properties and postsynaptic currents of granule cells in rat dentate gyrus. *Journal of Neurophysiology* **76**:1074–1088. DOI: <https://doi.org/10.1152/jn.1996.76.2.1074>, PMID: 8871221
- Lothman EW**, Stringer JL, Bertram EH. 1992. The dentate gyrus as a control point for seizures in the hippocampus and beyond. *Epilepsy Research. Supplement* **7**:301–313. PMID: 1334669
- Lu M**, Holliday LS, Zhang L, Dunn WA, Gluck SL. 2001. Interaction between aldolase and vacuolar H^+ -ATPase: evidence for direct coupling of glycolysis to the ATP-hydrolyzing proton pump. *The Journal of Biological Chemistry* **276**:30407–30413. DOI: <https://doi.org/10.1074/jbc.M008768200>, PMID: 11399750
- Lu Y**, Zhong C, Wang L, Wei P, He W, Huang K, Zhang Y, Zhan Y, Feng G, Wang L. 2016. Optogenetic dissection of ictal propagation in the hippocampal-entorhinal cortex structures. *Nature Communications* **7**:10962. DOI: <https://doi.org/10.1038/ncomms10962>, PMID: 26997093
- Lutas A**, Birnbaumer L, Yellen G. 2014. Metabolism regulates the spontaneous firing of substantia nigra pars reticulata neurons via K_{ATP} and nonselective cation channels. *The Journal of Neuroscience* **34**:16336–16347. DOI: <https://doi.org/10.1523/JNEUROSCI.1357-14.2014>, PMID: 25471572
- Lévesque M**, Herrington R, Hamidi S, Avoli M. 2016. Interneurons spark seizure-like activity in the entorhinal cortex. *Neurobiology of Disease* **87**:91–101. DOI: <https://doi.org/10.1016/j.nbd.2015.12.011>, PMID: 26721318
- Martin GM**, Yoshioka C, Rex EA, Fay JF, Xie Q, Whorton MR, Chen JZ, Shyng SL. 2017. Cryo-EM structure of the ATP-sensitive potassium channel illuminates mechanisms of assembly and gating. *eLife* **6**:e24149. DOI: <https://doi.org/10.7554/eLife.24149>, PMID: 28092267
- Masino SA**, Li T, Theofilas P, Sandau US, Ruskin DN, Fredholm BB, Geiger JD, Aronica E, Boison D. 2011. A ketogenic diet suppresses seizures in mice through adenosine A_1 receptors. *Journal of Clinical Investigation* **121**:2679–2683. DOI: <https://doi.org/10.1172/JCI57813>, PMID: 21701065
- Mercer RW**, Dunham PB. 1981. Membrane-bound ATP fuels the Na/K pump. Studies on membrane-bound glycolytic enzymes on inside-out vesicles from human red cell membranes. *The Journal of General Physiology* **78**:547–568. DOI: <https://doi.org/10.1085/jgp.78.5.547>, PMID: 6273495
- Mergenthaler P**, Lindauer U, Dienel GA, Meisel A. 2013. Sugar for the brain: the role of glucose in physiological and pathological brain function. *Trends in Neurosciences* **36**:587–597. DOI: <https://doi.org/10.1016/j.tins.2013.07.001>, PMID: 23968694
- Meyer M**, Kienzler-Norwood F, Bauer S, Rosenow F, Norwood BA. 2016. Removing entorhinal cortex input to the dentate gyrus does not impede low frequency oscillations, an EEG-biomarker of hippocampal epileptogenesis. *Scientific Reports* **6**:25660. DOI: <https://doi.org/10.1038/srep25660>, PMID: 27160925
- Michelson HB**, Wong RK. 1991. Excitatory synaptic responses mediated by GABA $_A$ receptors in the hippocampus. *Science* **253**:1420–1423. DOI: <https://doi.org/10.1126/science.1654594>, PMID: 1654594
- Miki T**, Liss B, Minami K, Shiuchi T, Saraya A, Kashima Y, Horiuchi M, Ashcroft F, Minokoshi Y, Roeper J, Seino S. 2001. ATP-sensitive K^+ channels in the hypothalamus are essential for the maintenance of glucose homeostasis. *Nature Neuroscience* **4**:507–512. DOI: <https://doi.org/10.1038/87455>, PMID: 11319559
- Miles R**, Wong RK, Traub RD. 1984. Synchronized afterdischarges in the hippocampus: contribution of local synaptic interactions. *Neuroscience* **12**:1179–1189. DOI: [https://doi.org/10.1016/0306-4522\(84\)90012-5](https://doi.org/10.1016/0306-4522(84)90012-5), PMID: 6090986

- Mody I**, Lambert JD, Heinemann U. 1987. Low extracellular magnesium induces epileptiform activity and spreading depression in rat hippocampal slices. *Journal of Neurophysiology* **57**:869–888. DOI: <https://doi.org/10.1152/jn.1987.57.3.869>, PMID: 3031235
- Mongiati LA**, Schinder AF. 2011. Adult neurogenesis and the plasticity of the dentate gyrus network. *European Journal of Neuroscience* **33**:1055–1061. DOI: <https://doi.org/10.1111/j.1460-9568.2011.07603.x>, PMID: 21395848
- Mourre C**, Widmann C, Lazdunski M. 1991. Specific hippocampal lesions indicate the presence of sulfonylurea binding sites associated to ATP-sensitive K^+ channels both post-synaptically and on mossy fibers. *Brain Research* **540**:340–344. DOI: [https://doi.org/10.1016/0006-8993\(91\)90533-2](https://doi.org/10.1016/0006-8993(91)90533-2), PMID: 1905175
- Murphy BM**, Engel T, Paucard A, Hatazaki S, Mouri G, Tanaka K, Tuffy LP, Jimenez-Mateos EM, Woods I, Dunleavy M, Bonner HP, Meller R, Simon RP, Strasser A, Prehn JH, Henshall DC. 2010. Contrasting patterns of Bim induction and neuroprotection in Bim-deficient mice between hippocampus and neocortex after status epilepticus. *Cell Death & Differentiation* **17**:459–468. DOI: <https://doi.org/10.1038/cdd.2009.134>, PMID: 19779495
- Neal EG**, Chaffe H, Schwartz RH, Lawson MS, Edwards N, Fitzsimmons G, Whitney A, Cross JH. 2009. A randomized trial of classical and medium-chain triglyceride ketogenic diets in the treatment of childhood epilepsy. *Epilepsia* **50**:1109–1117. DOI: <https://doi.org/10.1111/j.1528-1167.2008.01870.x>, PMID: 19054400
- Nichols CG**. 2006. K_{ATP} channels as molecular sensors of cellular metabolism. *Nature* **440**:470–476. DOI: <https://doi.org/10.1038/nature04711>, PMID: 16554807
- Owen OE**, Morgan AP, Kemp HG, Sullivan JM, Herrera MG, Cahill GF. 1967. Brain metabolism during fasting. *Journal of Clinical Investigation* **46**:1589–1595. DOI: <https://doi.org/10.1172/JCI105650>, PMID: 6061736
- Pan JW**, Bebin EM, Chu WJ, Hetherington HP. 1999. Ketosis and epilepsy: ^{31}P spectroscopic imaging at 4.1 T. *Epilepsia* **40**:703–707. DOI: <https://doi.org/10.1111/j.1528-1157.1999.tb00766.x>, PMID: 10368066
- Paul RJ**, Bauer M, Pease W. 1979. Vascular smooth muscle: aerobic glycolysis linked to sodium and potassium transport processes. *Science* **206**:1414–1416. DOI: <https://doi.org/10.1126/science.505014>, PMID: 505014
- Pelletier MR**, Pahapill PA, Pennefather PS, Carlen PL. 2000. Analysis of single K_{ATP} channels in mammalian dentate gyrus granule cells. *Journal of Neurophysiology* **84**:2291–2301. DOI: <https://doi.org/10.1152/jn.2000.84.5.2291>, PMID: 11067973
- Pfeifer HH**, Lyczkowski DA, Thiele EA. 2008. Low glycemic index treatment: implementation and new insights into efficacy. *Epilepsia* **49 Suppl 8**:42–45. DOI: <https://doi.org/10.1111/j.1528-1167.2008.01832.x>, PMID: 19049585
- Piatti VC**, Ewell LA, Leutgeb JK. 2013. Neurogenesis in the dentate gyrus: carrying the message or dictating the tone. *Frontiers in Neuroscience* **7**:50. DOI: <https://doi.org/10.3389/fnins.2013.00050>, PMID: 23576950
- Pierrefiche O**, Bischoff AM, Richter DW. 1996. ATP-sensitive K^+ channels are functional in expiratory neurones of normoxic cats. *The Journal of Physiology* **494 (Pt 2)**:399–409. DOI: <https://doi.org/10.1113/jphysiol.1996.sp021501>, PMID: 8842000
- Proks P**, Ashcroft FM. 2009. Modeling K_{ATP} channel gating and its regulation. *Progress in Biophysics and Molecular Biology* **99**:7–19. DOI: <https://doi.org/10.1016/j.pbiomolbio.2008.10.002>, PMID: 18983870
- Rheims S**, Minlebaev M, Ivanov A, Represa A, Khazipov R, Holmes GL, Ben-Ari Y, Zilberter Y. 2008. Excitatory GABA in rodent developing neocortex in vitro. *Journal of Neurophysiology* **100**:609–619. DOI: <https://doi.org/10.1152/jn.90402.2008>, PMID: 18497364
- Rowe IC**, Treherne JM, Ashford ML. 1996. Activation by intracellular ATP of a potassium channel in neurones from rat basomedial hypothalamus. *The Journal of Physiology* **490 (Pt 1)**:97–113. DOI: <https://doi.org/10.1113/jphysiol.1996.sp021129>, PMID: 8745281
- Rutecki PA**, Lebeda FJ, Johnston D. 1987. 4-Aminopyridine produces epileptiform activity in hippocampus and enhances synaptic excitation and inhibition. *Journal of Neurophysiology* **57**:1911–1924. DOI: <https://doi.org/10.1152/jn.1987.57.6.1911>, PMID: 3037040
- Sada N**, Lee S, Katsu T, Otsuki T, Inoue T. 2015. Epilepsy treatment. Targeting LDH enzymes with a stiripentol analog to treat epilepsy. *Science* **347**:1362–1367. DOI: <https://doi.org/10.1126/science.aaa1299>, PMID: 25792327
- Schmidt-Hieber C**, Jonas P, Bischofberger J. 2004. Enhanced synaptic plasticity in newly generated granule cells of the adult hippocampus. *Nature* **429**:184–187. DOI: <https://doi.org/10.1038/nature02553>, PMID: 15107864
- Shyng SL**, Nichols CG. 1998. Membrane phospholipid control of nucleotide sensitivity of K_{ATP} channels. *Science* **282**:1138–1141. DOI: <https://doi.org/10.1126/science.282.5391.1138>, PMID: 9804554
- Shyng SL**, Cukras CA, Harwood J, Nichols CG. 2000. Structural determinants of PIP_2 regulation of inward rectifier K_{ATP} channels. *The Journal of General Physiology* **116**:599–608. DOI: <https://doi.org/10.1085/jgp.116.5.599>, PMID: 11055989
- Simeone TA**, Simeone KA, Samson KK, Kim DY, Rho JM. 2013. Loss of the $K_v1.1$ potassium channel promotes pathologic sharp waves and high frequency oscillations in *in vitro* hippocampal slices. *Neurobiology of Disease* **54**:68–81. DOI: <https://doi.org/10.1016/j.nbd.2013.02.009>, PMID: 23466697
- Simeone TA**, Samson KK, Matthews SA, Simeone KA. 2014. In vivo ketogenic diet treatment attenuates pathologic sharp waves and high frequency oscillations in *in vitro* hippocampal slices from epileptic $K_v1.1\alpha$ knockout mice. *Epilepsia* **55**:e44–e49. DOI: <https://doi.org/10.1111/epi.12603>, PMID: 24702645
- Sinha SR**, Saggau P. 2001. Imaging of 4-AP-induced, GABA_A-dependent spontaneous synchronized activity mediated by the hippocampal interneuron network. *Journal of Neurophysiology* **86**:381–391. DOI: <https://doi.org/10.1152/jn.2001.86.1.381>, PMID: 11431518

- Skarnes WC**, Rosen B, West AP, Koutsourakis M, Bushell W, Iyer V, Mujica AO, Thomas M, Harrow J, Cox T, Jackson D, Severin J, Biggs P, Fu J, Nefedov M, de Jong PJ, Stewart AF, Bradley A. 2011. A conditional knockout resource for the genome-wide study of mouse gene function. *Nature* **474**:337–342. DOI: <https://doi.org/10.1038/nature10163>, PMID: 21677750
- Song Z**, Levin BE, McArdle JJ, Bakhos N, Routh VH. 2001. Convergence of pre- and postsynaptic influences on glucosensing neurons in the ventromedial hypothalamic nucleus. *Diabetes* **50**:2673–2681. DOI: <https://doi.org/10.2337/diabetes.50.12.2673>, PMID: 11723049
- Spencer SS**, Spencer DD. 1994. Entorhinal-hippocampal interactions in medial temporal lobe epilepsy. *Epilepsia* **35**:721–727. DOI: <https://doi.org/10.1111/j.1528-1157.1994.tb02502.x>, PMID: 8082614
- Stafstrom CE**, Ockuly JC, Murphree L, Valley MT, Roopra A, Sutula TP. 2009. Anticonvulsant and antiepileptic actions of 2-deoxy-D-glucose in epilepsy models. *Annals of Neurology* **65**:435–447. DOI: <https://doi.org/10.1002/ana.21603>, PMID: 19399874
- Sun HS**, Feng ZP, Miki T, Seino S, French RJ. 2006. Enhanced neuronal damage after ischemic insults in mice lacking Kir6.2-containing ATP-sensitive K⁺ channels. *Journal of Neurophysiology* **95**:2590–2601. DOI: <https://doi.org/10.1152/jn.00970.2005>, PMID: 16354731
- Sun HS**, Feng ZP. 2013. Neuroprotective role of ATP-sensitive potassium channels in cerebral ischemia. *Acta Pharmacologica Sinica* **34**:24–32. DOI: <https://doi.org/10.1038/aps.2012.138>, PMID: 23123646
- Tanner GR**, Lutas A, Martínez-François JR, Yellen G. 2011. Single K_{ATP} channel opening in response to action potential firing in mouse dentate granule neurons. *Journal of Neuroscience* **31**:8689–8696. DOI: <https://doi.org/10.1523/JNEUROSCI.5951-10.2011>, PMID: 21653873
- Thiele EA**. 2003. Assessing the efficacy of antiepileptic treatments: the ketogenic diet. *Epilepsia* **44 Suppl 7**:26–29. DOI: <https://doi.org/10.1046/j.1528-1157.44.s7.4.x>, PMID: 12919336
- Ting JT**, Daigle TL, Chen Q, Feng G. 2014. Acute brain slice methods for adult and aging animals: application of targeted patch clamp analysis and optogenetics. *Methods in Molecular Biology* **1183**:221–242. DOI: https://doi.org/10.1007/978-1-4939-1096-0_14, PMID: 25023312
- Uhlemann ER**, Neims AH. 1972. Anticonvulsant properties of the ketogenic diet in mice. *The Journal of Pharmacology and Experimental Therapeutics* **180**:231–238. PMID: 5010672
- Uva L**, Librizzi L, Wendling F, de Curtis M. 2005. Propagation dynamics of epileptiform activity acutely induced by bicuculline in the hippocampal-parahippocampal region of the isolated Guinea pig brain. *Epilepsia* **46**:1914–1925. DOI: <https://doi.org/10.1111/j.1528-1167.2005.00342.x>, PMID: 16393157
- Voskuyl RA**, Albus H. 1985. Spontaneous epileptiform discharges in hippocampal slices induced by 4-aminopyridine. *Brain Research* **342**:54–66. DOI: [https://doi.org/10.1016/0006-8993\(85\)91352-6](https://doi.org/10.1016/0006-8993(85)91352-6), PMID: 2994823
- Walther H**, Lambert JD, Jones RS, Heinemann U, Hamon B. 1986. Epileptiform activity in combined slices of the hippocampus, subiculum and entorhinal cortex during perfusion with low magnesium medium. *Neuroscience Letters* **69**:156–161. DOI: [https://doi.org/10.1016/0304-3940\(86\)90595-1](https://doi.org/10.1016/0304-3940(86)90595-1), PMID: 3763042
- Watts AE**, Jefferys JG. 1993. Effects of carbamazepine and baclofen on 4-aminopyridine-induced epileptic activity in rat hippocampal slices. *British Journal of Pharmacology* **108**:819–823. DOI: <https://doi.org/10.1111/j.1476-5381.1993.tb12884.x>, PMID: 8467367
- Weissinger F**, Buchheim K, Siegmund H, Heinemann U, Meierkord H. 2000. Optical imaging reveals characteristic seizure onsets, spread patterns, and propagation velocities in hippocampal-entorhinal cortex slices of juvenile rats. *Neurobiology of Disease* **7**:286–298. DOI: <https://doi.org/10.1006/nbdi.2000.0298>, PMID: 10964601
- Whittington MA**, Traub RD, Jefferys JG. 1995. Erosion of inhibition contributes to the progression of low magnesium bursts in rat hippocampal slices. *The Journal of Physiology* **486 (Pt 3)**:723–734. DOI: <https://doi.org/10.1113/jphysiol.1995.sp020848>, PMID: 7473233
- Yamada K**, Ji JJ, Yuan H, Miki T, Sato S, Horimoto N, Shimizu T, Seino S, Inagaki N. 2001. Protective role of ATP-sensitive potassium channels in hypoxia-induced generalized seizure. *Science* **292**:1543–1546. DOI: <https://doi.org/10.1126/science.1059829>, PMID: 11375491
- Yu EP**, Dengler CG, Frausto SF, Putt ME, Yue C, Takano H, Coulter DA. 2013. Protracted postnatal development of sparse, specific dentate granule cell activation in the mouse hippocampus. *Journal of Neuroscience* **33**:2947–2960. DOI: <https://doi.org/10.1523/JNEUROSCI.1868-12.2013>, PMID: 23407953
- Yudkoff M**, Daikhin Y, Melø TM, Nissim I, Sonnewald U, Nissim I. 2007. The ketogenic diet and brain metabolism of amino acids: relationship to the anticonvulsant effect. *Annual Review of Nutrition* **27**:415–430. DOI: <https://doi.org/10.1146/annurev.nutr.27.061406.093722>, PMID: 17444813
- Yudkoff M**, Daikhin Y, Horyn O, Nissim I, Nissim I. 2008. Ketosis and brain handling of glutamate, glutamine, and GABA. *Epilepsia* **49 Suppl 8**:73–75. DOI: <https://doi.org/10.1111/j.1528-1167.2008.01841.x>, PMID: 19049594
- Zawar C**, Plant TD, Schirra C, Konnerth A, Neumcke B. 1999. Cell-type specific expression of ATP-sensitive potassium channels in the rat hippocampus. *The Journal of Physiology* **514 (Pt 2)**:327–341. DOI: <https://doi.org/10.1111/j.1469-7793.1999.315ae.x>, PMID: 9852317
- Zhang CL**, Dreier JP, Heinemann U. 1995. Paroxysmal epileptiform discharges in temporal lobe slices after prolonged exposure to low magnesium are resistant to clinically used anticonvulsants. *Epilepsy Research* **20**:105–111. DOI: [https://doi.org/10.1016/0920-1211\(94\)00067-7](https://doi.org/10.1016/0920-1211(94)00067-7), PMID: 7750506
- Zielke HR**, Zielke CL, Baab PJ. 2009. Direct measurement of oxidative metabolism in the living brain by microdialysis: a review. *Journal of Neurochemistry* **109 Suppl 1**:24–29. DOI: <https://doi.org/10.1111/j.1471-4159.2009.05941.x>, PMID: 19393005